Laboratory of Microbiology

Bacterial genetics group

Synthetic methanotrophy in *Escherichia coli* for ruminant biofilters

MSc Thesis

Written by:

Kanyn Morris Pouw

student ID: 1027422

Supervised by:

Eric Vossen

Nico Claassens

Examiners:

Nico Claassens

Serve Kengen

15-01-2024

Abstract

Ruminant emissions are responsible for a significant portion of the anthropogenic greenhouse gases that cause global warming. Methane emissions from cows are diffuse and difficult to treat, however, several solutions have been proposed which could reduce low (v/v) methane streams emitted from cattle up to ~30%. The novel Cattlelyst biofilter proposed by the Wageningen University & Research international Genetic Engineering Machine competition team is designed is to collect and convert the methane and ammonia emitted from cattle by means of a hood system and two genetically modified organisms under three layers of safety mechanisms. The goal is to engineer *Escherichia coli* into a suitable synthetic methanotroph. In this thesis synthetic methanotrophy was attempted to be expressed in a suitable methanotrophic strain SM1 or C1Saux. The resulting products are one pSEVA2610-sMMO plasmid containing the subunits of sMMO with a duplication in the *mmoX gene*. The other chaperone plasmid could not be achieved and methylotrophic growth of the SM1 and C1Saux strain was not shown. In the end the hypothesis has neither been confirmed or rejected. Synthetic methanotrophy for biofilters is becoming an increasingly relevant technology for tackling low concentrations of methane as multiple technological advances are made as explored in this thesis. It is expected that improvements in biofilter design such as concentrating methane in a hood, porous packing material, and specific cultures which are engineerable could make biofilters a useful tool in achieving the global methane pledge.

Table of Contents

Introduction

Societal importance of methane

Natural gas consists for the majority out of methane, CH_4, a hydrocarbon and the simplest alkane (Favre & Powell, 2013; Howarth, 2014). Methane can originate from natural sources: pyrogenic such as wildfires or thermogenic geological processes or biogenic such as anaerobic fermentation of biomass by methanogens (Kirschke et al., 2013). Anthropogenic methane accounts for 60% of methane emissions and is produced by the energy sector, waste streams and agriculture (Myrhe & Shindell, 2013). Over half of these anthropogenic emissions are diffuse and contain a methane concentration less than 3% (v/v), which is below the 5% threshold that needs to be maintained for proper thermal oxidation (La et al., 2018). After methane is produced it rises to the atmosphere where it acts as a greenhouse gas (GHG) by trapping infrared heat radiation (Burch & Williams, 1962). The main global methane sink (90%) is in the atmosphere where methane is oxidized by hydroxyl radicals (Kirschke et al., 2013). Despite residing in the atmosphere for only a decade, methane is a potent GHG. Over a duration of 20 years methane absorbs as much as 84 times the CO_2 equivalent of infrared heat radiation (Vallero, 2019). The intergovernmental panel on climate change determined that the average global temperature has risen by ~1°C in 2017 since preindustrial levels**.** Of the 1°C rise in average global temperature about 25% of the net rise is attributed to methane (van Amstel, 2012). A collective effort of over 100 countries called the Global Methane Pledge aims to reduce global warming with 0.2°C by 2050 through mitigating methane emissions by 30% (Birol, 2021). The distribution of major anthropogenic sources of methane emissions are shown in figure 1 (Olivier & Peters, 2020). Since a significant portion of methane emissions originates from ruminants, understanding how methane is formed in cattle is necessary for finding a solution.

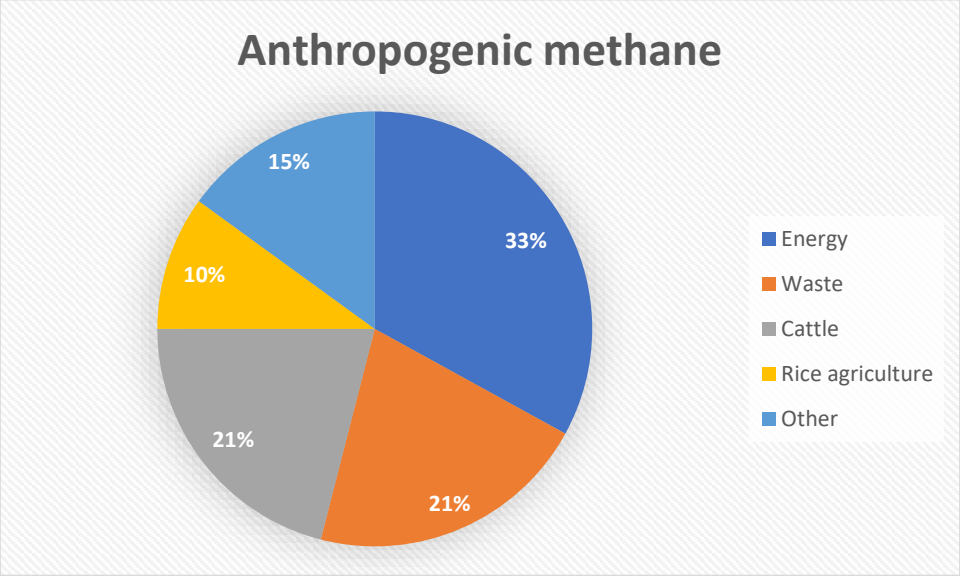

Figure 1. Distribution of anthropogenic sources of methane.

Methanogenesis in cattle

The cattle industry already has a significant impact on the environment through their emissions and this impact is anticipated to increase in the coming years. There is a disparity between the available food in 2010 and the food required to feed the human population in 2050. An additional 3 billion people will need to be fed by 2050 and as incomes rise the demand for animal-based food increases under the business-as-usual model (Ranganathan et al., 2018). This “business as usual” model is problematic since the rise in demand for animal-based foods leads to more cattle producing methane. A single dairy cow can generate three tons of CO_2 equivalents every year (van Lingen et al., 2021). The source of this methane is predominantly the rumen (89%) and only partially the small intestine (11%) (Getabalew et al., 2019). In these regions the dietary plant cell wall polysaccharides are broken down by microbes into among others hydrogen (Miller & Wolin, 2001). Hydrogen is an important intermediate for methane in the rumen fermentation (Hungate, 1967). Accumulation of hydrogen is detrimental for the health of cows and several hydrogen sinks exist to avoid this. Of the existing hydrogen sinks, methane and ammonia are of importance for GHG (Pereira et al., 2022). The organisms responsible for methane production are methanogenic archaea (Morgavi et al., 2010). Methanogenic microbes produce methane through two biochemical pathways: through acetate decarboxylation and the reduction of carbon dioxide. In the rumen most methane is produced from hydrogen reducing carbon dioxide into water and methane $4\ H_2 + C\ O_2 \rightarrow 2\ H_2O + CH_4$ (Wilkinson, 2012). Interfering with the reduction of carbon dioxide can be an interesting approach towards decreasing the methane production and redirecting hydrogen metabolism (Ungerfeld, 2020).

State of the art technology for methane emissions

Multiple technological solutions are pursued to reduce the methane emissions from ruminants, and most solutions involve a trade-off between implementation difficulty, cost-effectiveness, and animal welfare. One of these solutions is through food additives that interfere with the reduction of carbon dioxide. Bovaer® is an EU approved feed additive that reduces methane emissions by about 30% (Bampidis et al., 2021). The interaction of the feed additive works by disrupting the methanogenesis pathway. The MCR enzyme necessary to complete methanogenesis gets inhibited and overall methane formation is decreased (Johnson et al., 2011). The implementation of food additives is straightforward but put an annual burden of costs on the farmer plus the hydrogen sink can produce other harmful compounds such as NH_4+ and H_2S (Pereira et al., 2022). The company ZELP has taken a different approach by developing a “cattle harness” that directly catches methane from belching and converts up to 60% of the emitted methane (Norris et al., 2023). The mechanism uses a patented energy recovery-system to facilitate catalytic methane oxidation, resulting in CO_2 and water vapor (Lee & Trimm, 1995). However, making cows wear harnesses on their faces has been shown to hinder social grooming (allogrooming**)** which negatively impacts animal welfare (Buijs et al., 2023; Val-Laillet et al., 2009). Another approach to tackle emissions is by genetic variation of cows. Studies have shown that around 30 per cent of methane variation between cows is heritable and depends on their genetic profile (van Breukelen et al., 2022). If economic weight is put on the breeding goal, then selective breeding can result in reduction of methane intensity by about 24% by 2050 (de Haas et al., 2021). Finally, there is the approach of methane biofiltration with immobilized methane-oxidizing bacteria (MOB). The MOB consortium was fed a 1% (v/v) methane airstream that according to Henry’s law corresponds with a dissolved methane concentration of ~20 µM at 15 °C and 1 atm (Cookney et al., 2016). Because methane has gas-liquid mass transfer limitations larger biofilters are needed which hinder economic viability (Melse & Van Der Werf, 2005). One of the ways to improve biofilter activity is biofilter design, such as optimizing packing material. Experiments testing biofilter packing material found that fly ash

ceramsite is 33% more effective than suspended cells as it reached an elimination capacity of 4.628 g h^1 m^3 and the lowest average outlet reached 0.78% (v/v) methane (Sun et al., 2020). Another problem with current biofilters is that they consist of a consortium of methane oxidising bacteria and the biofilter performance can vary over time depending on biomass concentration (Kim et al., 2014). One of the proposed solutions to improve biofilters is to use a specific culture (Cáceres et al., 2017).

Cattlelyst

In 2021 the team of Wageningen University & Research (WUR) participated in the international Genetically Engineered Machine (iGEM) competition (Bakker et al., 2021). The project called Cattlelyst aims to tackle methane and nitrogen emissions from cattle, two major greenhouse gasses and pollutants (Dijkstra et al., 2011). The approach to tackle these emissions is by using a hood system to collect ruminant emissions and direct airflow through a biofilter containing genetically modified microorganisms as can be seen on figure 2 (Aarnink et al., 2011). The biofilter is build on 3 major pillars: safety, ammonia removal and methane conversion (Bakker et al., 2021). The biofilter contains two genetically modified organisms: *Escherichia coli* and *Pseudonomas putida,* that according to Genetically Modified Organism (GMO) legislation from the European commission, must not be released into the environment and neither end up in food or feed (Arpaia et al., 2015; Spranger, 2015). For the first pillar several layers of safety are designed. A methane-dependant kill switch that upon detecting low methane concentrations produces toxins and kills the *E. coli* host. A proximity-dependent kill switch that senses cell densities, killing both *E. coli* and *P. putida* with toxin production upon low cell densities. And build in co-dependency, by making both strains nutrient-dependent for amino acids and a carbon source. The second pillar of the biofilter, converts ammonia (NH3) to harmless dinitrogen gas (N2). This process is enabled by a novel technology called heterotrophic nitrification aerobic denitrification (HNAD). In the HNAD pathway denitrification is coupled to nitrification (Chen & Ni, 2011). And the third pillar aims to convert methane into biomass and CO_2 with a novel synthetic methanotroph (Bennett et al., 2021).

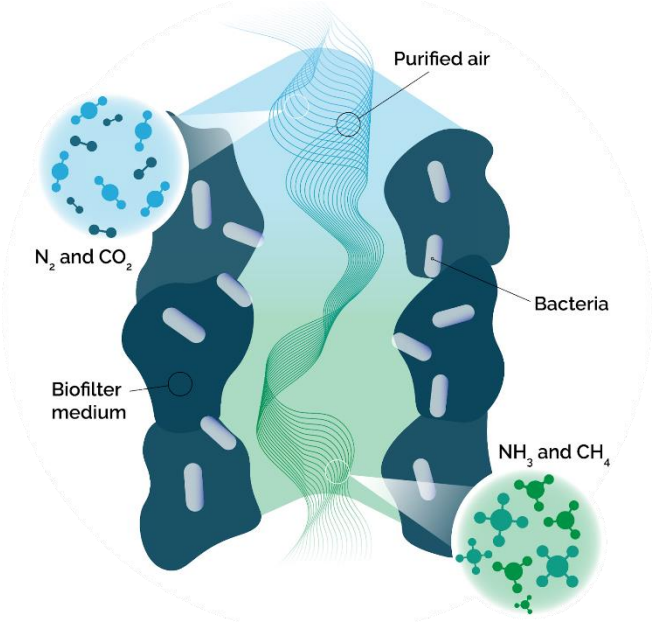

Figure 2. Simplified overview showing the components of the Cattlelyst filter system. Air excreted by ruminants is taken up by the hood system and is then guided through the biofilter. The biofilter contains genetically modified bacteria that are made able to convert methane and ammonia into CO_2 and N_2 (Bakker et al., 2021).

Methanotrophy in nature

Methanotrophy, the consumption of methane as carbon or energy source through bacterial metabolism, can occur aerobically and anaerobically. Aerobic methanotrophs found so far belong to one of three groups: the type I and X Gammaproteobacteria (found at low methane ppm and utilizes the RuMP pathway) or type II Alphaproteobacteria (utilizes the serine pathway) (Dedysh & Knief, 2018). Anaerobic methanotrophs are found in among others deep-sea sediments where they remove ~80% of produced methane (Reeburgh, 2007). These methanotrophs belong to the class anaerobic methanotrophic archaea (ANME) (Hinrichs et al., 1999). Anaerobic methanotrophs reduce iron, sulfate, manganese, nitrite or nitrate and couple this to methane oxidation (Guerrero-Cruz et al., 2021). In aerobic methanotrophs one-carbon(C1) metabolism starts by converting methane to methanol by a methane monooxygenase (Ross & Rosenzweig, 2017). In the next step methanol is oxidized by a methanol dehydrogenase (Mdh) to formaldehyde by one of three different methanol dehydrogenases that oxidize differently and are either pyrroloquinoline quinone (PQQ)-containing, NAD-dependent or O_2-dependent (Anthony, 1982; Krog et al., 2013; Yurimoto et al., 2011). Formaldehyde can be metabolised through one of four natural pathways: the xylulose monophosphate (XuMP) pathway, the ribulose bisphosphate (RuBP) pathway, the serine cycle, or the ribulose monophosphate (RuMP) pathway as can be seen in figure 3 (Gregory et al., 2022a). The natural methanotrophs are well understood in their metabolism but are currently limited in their application due to slow growth, a narrow product spectrum and few genetic tools (Cotton et al., 2020; Stolyar et al., 1999).

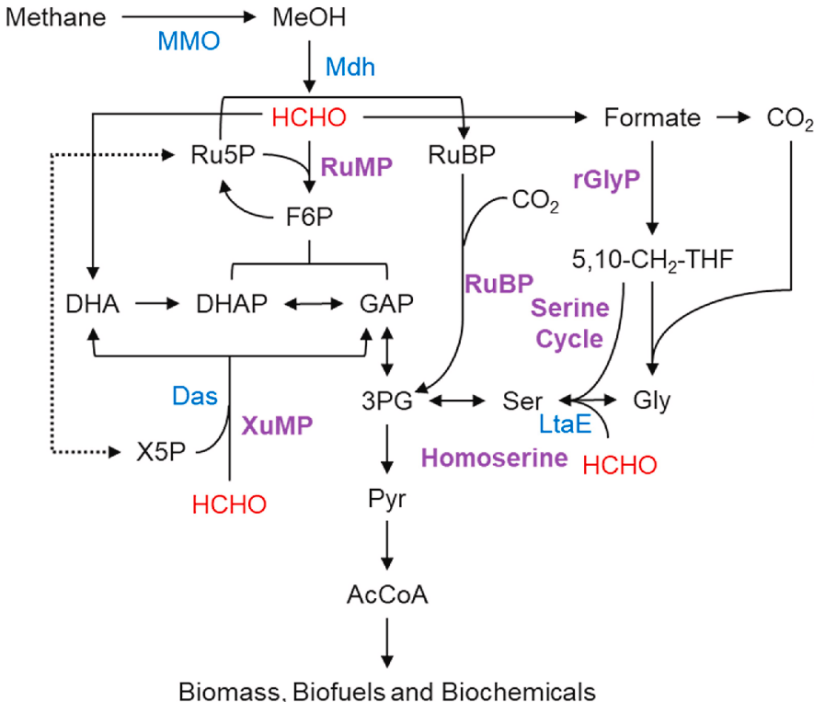

Figure 3. Aerobic pathways of methane metabolism. Purple colour indicates the native metabolic pathways, blue colour indicates key enzymes and in red is the intermediate formaldehyde entering the pathways. Abbreviations are as follows: AcCoA, acetyl-coA; Das, dihydroxyacetone synthase; DHA, dihydroxyacetone; DHAP, dihydroxyacetone phosphate; Fd, ferredoxin; F6P, fructose 6-phosphate; GAP, glyceraldehyde-3-phosphate; HCHO, formaldehyde; LtaE, threonine aldolase; Mcr, Methyl-coenzyme M reductase; Mdh, methanol dehydrogenase; MeOH, methanol; MMO, methane monooxygenase; MTI, methyltransferase I; MTII, methyltransferase II; 3 PG, 3-phosphoglycerate; Pyr, pyruvate; rGlyP, reductive glycine pathway; RuBP, ribulose bisphosphate; RuMP, ribulose monophosphate; Ru5P, ribulose-5-phosphate; 5,10-CH_2-THF, 5,10-methylene tetrahydrofolate; X5P, xylulose-5-phosphate; XuMP, xylulose monophosphate. Image source is from (Gregory et al., 2022).

Synthetic methylotrophy

Synthetic methylotrophy is a field that aims to utilise reduced one-carbon molecules (e.g., methane, methanol, formaldehyde and formate) as feedstock for non-methylotrophic hosts while retaining biotechnological relevance (Heux et al., 2018). One-carbon based feedstocks offer many advantages as they are widely available from different sources, do not compete with food security, can be made from CO_2 using renewable energy, and used carbon neutrally in fermentation processes for biochemicals, biofuels or biomass (Cotton et al., 2020; Li & Tsang, 2018). An industrial workhorse such as *Escherichia coli* is a well characterized organism that can be used as a cell factory in fermentation processes (Valle & Bolívar, 2021). *E. coli* has been intensively characterized and is the most studied microorganism worldwide with well-defined metabolic pathways, genetic tools and a fast doubling time(~20 min) (Gibson et al., 2018; Idalia & Bernardo, 2017). These qualities make *E. coli* a chassis fit for metabolic engineering (Woo et al., 2019). Major strides have been made in understanding the complexity of synthetic methylotrophy (Singh et al., 2022). Promising synthetic methylotrophic *E. coli* proof of concept strains able to utilise formaldehyde and methanol as feedstock have been established.

A novel methylotrophic strain is the SM1 strain than can utilize methanol its only carbon source for growth (Chen et al., 2020). The synthetic methylotrophic SM1 strain was made in *E. coli* K-12 BW25113 by introducing the RuMP pathway through disruption of the pentose phosphate pathway (PPP) (Grenier et al., 2014). First *rpiAB* was deleted and two variants of methanol metabolic enzymes were incorporated. The genes that initially incorporated the RuMP pathway into the genome were two synthetic operons containing: Two *Mdh* (*Cupriavidus necator)*, one *hps* (*Bacillus methanolicus)* and one *hps* (*Methylomicrobium burytense)*, two *phi* (*Methylobacillus flagellates)*, *tkt* (*Methylococcus capsulatus*, and *tal* from *Klebsiella pneuomniae)*. These genetic alterations together with laboratory evolution made the cells auxotrophic for methanol, requiring the addition of both methanol and xylose for growth. Afterwards ensemble modelling for robust analysis (EMRA) suggested flux improvement of the pathway through expressing *gapC* from *E. coli BL21* and deletion of lower glycolysis enzymes *pfkA* and *gapA*. Then through reintroducing *rpiA* and laboratory evolution this synthetic methylotrophic strain is able to utilize methanol as sole carbon source (figure 4). The many rounds of laboratory evolution resulted in mutations/deletions/duplications in 23 genes related to central carbon metabolism and regulation that results in increased flux through the RuMP pathway. A 4-fold copy number variation (CNV) of the insertion sequence was found that is hypothesized by authors for an improved growth rate on methanol (Chen et al., 2020). The resulting SM1 strain is reported to have a long lag phase, attributed partially to the DNA-Protein Crosslinking (DPC) problem from formaldehyde when inoculated from a stationary phase (Nakamura & Nakamura, 2020). This strain has shown growth on a methanol concentration range from 50 mM to 1.2 M. While having optimal growth on a methanol concentration of 400 mM. The SM1 strain only uses methanol as carbon source and is reported to have a doubling time of 8 hours with a maximum OD_{600} of 2 (Chen et al., 2020). This growth rate is comparable to native methylotrophs such *Pichia pastoris* (Moser et al., 2017). Culturing *E. coli* on just methanol as carbon source is a big milestone and has major potential for sustainable production. However, the conditions in the biofilter can be variable and cell regeneration might not keep up with cell death at low methane concentrations so an additional synthetic methylotroph should be considered.

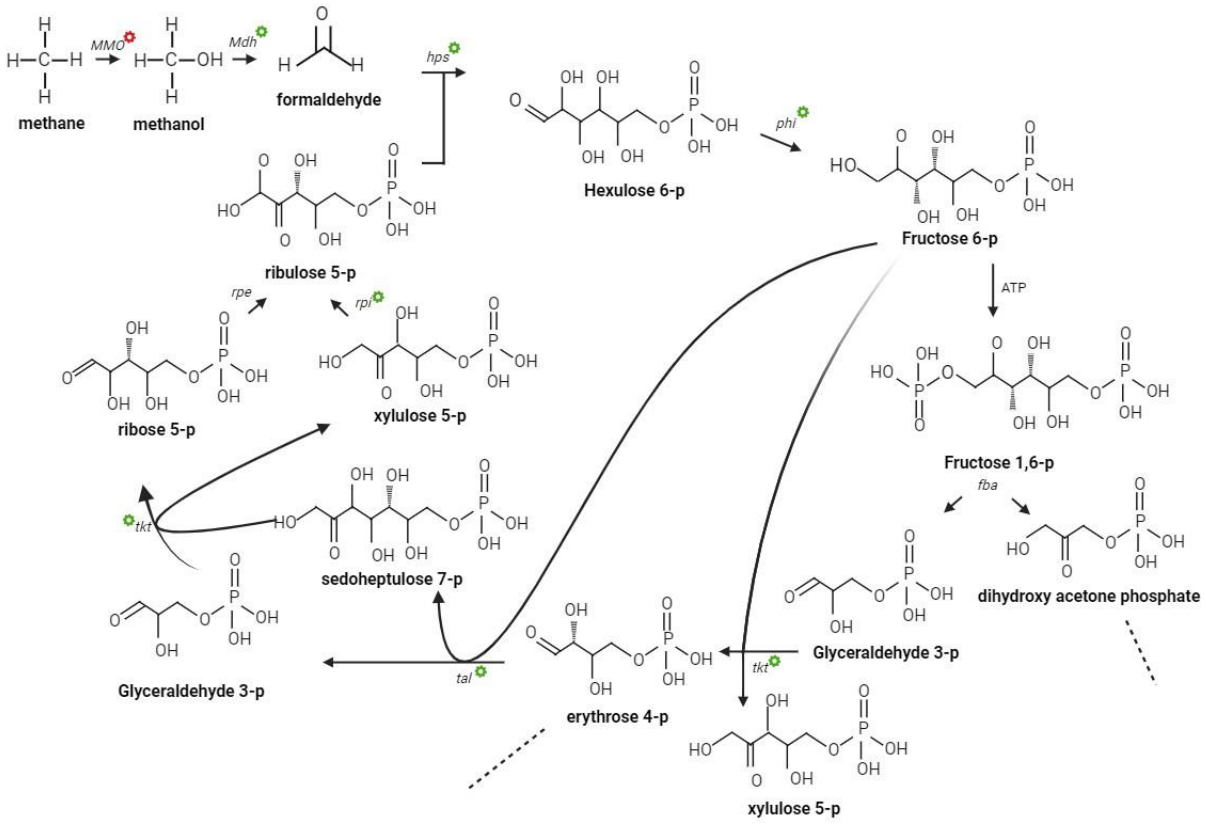

Figure 4. The RuMP pathway built in SM1 with a suggested addition of the MMO enzyme to convert methane. The skeletal structures are labelled in bold. Each arrow has the main enzyme next to it and represent reactions. Green gears indicate the enzymes that have been added to complete the pathway. The dashed lines show exit points for metabolites. The abbreviations used are: MMO, methane monooxygenase; Mdh, methanol dehydrogenase; hps, hexulose-6-phosphate synthase; phi, 6-phospho-3-hexuloisomerase; ATP, adenosine triphosphate; fba, fructose-1,6-bisphosphate aldolase; tkt, transketolase; tal, transaldolase; rpi, ribose-5-phosphate isomerase; rpe, ribulose-phosphate 3-epimerase. This image compiles RuMP pathway images from (Chen et al., 2020; Singh et al., 2022).

Another novel synthetic methylotrophic strain is the C1Saux strain (Yishai et al., 2017). This strain is auxotrophic for serine metabolism and requires formate to grow biomass. This auxotrophy results in the C1Saux strain being for 2-3% of its biomass dependant on formate assimilation (Neidhardt et al., 1990). This C1Saux strain produces serine through the reductive glycine (rGly) pathway. The rGly pathway is not cyclic, has limited interaction with central metabolism and efficiently converts two formate molecules with CO_2 to produce serine. The rGly pathway starts with the enzyme FTL coupling formate to tetrahydrofolate (THF) and creating 10-formyl-THF. The enzyme FolD reduces 10-formyl-THF to 5,10-methylene-THF (Bar-Even, 2016). In the reductive glycine pathway, the glycine cleave system can be reversed to combine 5,10-methylene-THF with NH3 and CO2 to create serine. Serine can then be deaminated to pyruvate which is used for biomass. The metabolism of formate and proposed metabolism of methane can be viewed in figure 5. The C1Saux strain was made by making *E. coli* MG1655 auxotrophic for serine by deleting the genes for glycine cleavage *Δ*glyA *Δ*gcvTHP and the genes for serine biosynthesis *ΔserA, ΔgcvTHP*. The auxotrophic strain was then made capable of metabolising formate by improving the reductive glycine pathway by overexpressing the genes *FTL, FolD,* and *GlyA* (Yishai et al., 2017). The achieved C1Saux strain is able to grow to an OD_{600} of 1.8 and doubles every 1.6 h on M9 minimal media with 10 mM glucose and 5 mM formate. The C1Saux strain and SM1 strain show that the RuMP and rGly pathway can be implemented and used in an industrial relevant organism such as *E. coli*. The next logical step would be for these strains to convert and use methane as carbon source as this could make for an engineerable synthetic methanotroph.

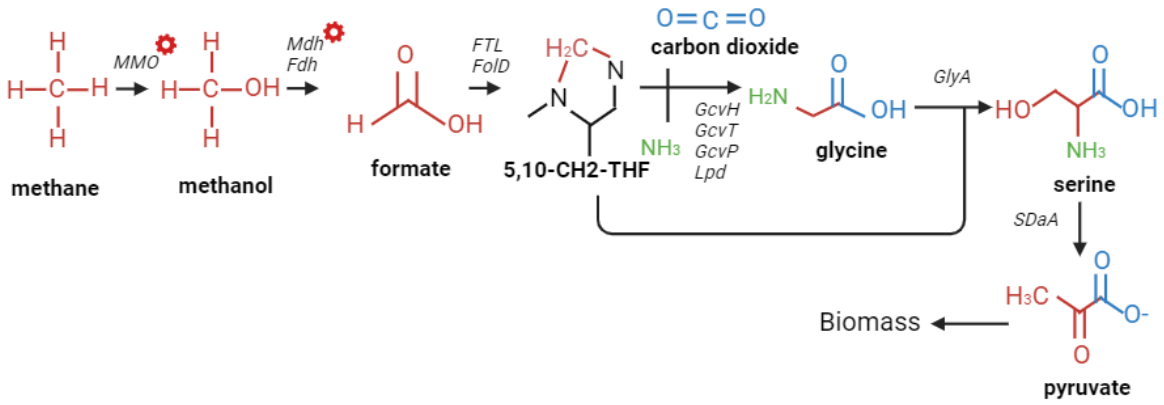

Figure 5. The reductive glycine pathway with additional reactions from proposed enzymes methane monooxygenase (MMO) and methanol dehydrogenase (Mdh) to convert methane. Red indicates where formate enters the pathways, blue indicates where CO_2 enters the pathways and green indicates the ammonia/nitrogen. The abbreviations used are: MMO, methane monooxygenase; Mdh, methanol dehydrogenase; Fdh, formaldehyde dehydrogenase; FTL, formate tetrahydrofolate; FolD, bifunctional methenyl tetrahydrofolate cyclohydrolase/dehydrogenase; GcvH, lipoyl carrier protein; GcvT, amino methyltransferase; GcvP, glycine dehydrogenase (decarboxylating); Lpd, dihydrolipoyl dehydrogenase; GlyA, serine hydroxy methyltransferase; SDaA, serine deaminase. Image adapted from (Yishai et al., 2018)

Aim of the project

The overarching goal of the project is to build the novel Cattlelyst biofilter with GMOs able to convert ammonia to nitrogen gas and methane to CO_2. The Cattlelyst biofilter requires a synthetic methanotroph that can convert methane for the co-culture with *Pseudomonas putida* and is accessible to build in safety mechanisms to contain the GMOs. The aim of the project is to build a synthetic methanotroph in *E. coli* for the Cattlelyst biofilter. A synthetic methanotroph in *E. coli* requires two things: a methane monooxygenase (MMO) to convert methane to methanol and a suitable synthetic methylotrophic pathway for the metabolism of methanol to biomass (Nguyen et al., 2016). There are two versions of MMO that have been expressed heterologously by Bennett et al. (2021) and Kim et al. (2019) and two milestone synthetic methylotrophic strains have been made available by Chen et al. (2020) and Yishai et al. (2017). The hypothesize is that the expression of soluble methane monooxygenase with either the RumP pathway of the SM1 strain or the reductive glycine pathway of C1Saux strain with an additional methanol dehydrogenase should allow *Escherichia coli* to consume methane as carbon source.

To accomplish synthetic methanotrophy a soluble form of the enzyme methane monooxygenase (MMO) is required (Nguyen et al., 2016). A soluble pMMO-mimetic enzyme was designed using a soluble human heavy-chain ferritin (huHF) scaffold to preserve the catalytic structure of the pMMO domains from *Methylococcus capsulatus* (bath). The best subunit structure, pMMO-m3, resulted in stable soluble protein with activity comparable to wild-type pMMO. pMMO is interesting for biofilter applications because of the higher affinity to methane than sMMO and allowing some methanotrophs to grow on 10-100 ppm methane (Baani & Liesack, 2008). However, the enzyme activity was measured *in vitro* and no *in vivo* results have been shown for this enzyme (Kim et al., 2019). To establish *in vivo* synthetic methane oxidation the Bennett et al. (2021) expressed sMMO instead. Functional and soluble sMMO expression from *Methylococcus capsulatus* was achieved in *E. coli* by overexpression of native *GroESL2* and introducing the sMMO subunits (*mmoX*YZBDC) with its cognate *GroESL* chaperone from *M. capsulatus*. The resulting enzymatic methanol productivity reached near 100 mg·gCDW·h. The expression system for the NADH dependant sMMO was then used in an *E. coli* strain (Δ*frmA*Δ*pgi* + pUD11) that produces acetone from glucose and methanol, resulting in the first synthetic methanotroph (Bennett et al., 2021; Bennett et al., 2018; Bermejo et al., 1998).

The published sMMO expression set-up can also be used in a suitable synthetic methylotrophic organism to convert methane to biomass and sustain the Cattlelyst biofilter. For the plasmid expression two plasmids are designed. To express sMMO all the subunits should be expressed as if they were on the same operon. To achieve stable and soluble sMMO expression two sets of chaperones are required, the cognate *GroESL-2* from *M. capsulatus* (Bath) and overexpressed *E. coli GroESL* (Bennett et al., 2021). The approach is to build two plasmids containing all the parts required for heterologous sMMO expression. One plasmid contains the operon of sMMO with the functional subunits *mmoXYZ* hydroxylase*, mmoBD* regulatory proteins and *mmoC* reductase from *M. capsulatus* expressed using the araBAD promoter system in a medium copy number plasmid (p15A ORI) on a pSEVA2610 backbone with kanamycin resistance. The other plasmid contains chaperones *GroESL* from *E. coli* and the *GroESL-2* from *M. capsulatus* are expressed constitutively by the J231XX promotor additionally with Mdh from *B*. *stearothermophilus* on a medium copy number plasmid (pBR322 ORI) with a pSEVA391 backbone containing chloramphenicol resistance. These plasmids when transformed together should replicate the two-plasmid set-up used by Bennett et al. (2021) and result in the functional expression of sMMO. The expressed MMO enzyme enables the oxidation of methane to methanol by use of NADH as electron source (Wang et al., 2014). The sMMO enzyme functionality can be tested for methanol production by gas chromatography when incubated with methane. The methanol produced by sMMO can also be used for biomass, with this read-out the SM1 and C1Saux strains can act as sensors.

The synthetic methylotrophic strains SM1 and C1Saux as shown by Chen et al. (2020) and Yishai et al. (2017) are able to grow on reduced C1 substrates using their respective RuMP or rGly pathway. To allow the C1Saux to grow on formate derived from methanol the enzyme Mdh from *Bacillus stearothermophilus* is added to the strain from the published plasmid pZASSC-rbsC-bsMDH (Wenk et al., 2020). To identify which strain is most suitable for the biofilter the SM1, C1Saux and C1Saux+BsMdh strains are grown over a 96-hours period on glucose and different methanol and formaldehyde concentrations during which the OD_{600} is measured over time on a platereader. The results of growth on different carbon source concentrations could help in defining the conditions in which carbon source levels are limiting biomass accumulation. The strain with the lowest methanol requirement to grow could function as a sensor strain with a lower demand scenario to determine if sMMO is converting methane.

Materials and methods

Cloning design

The cloning strategy to build the sMMO expression plasmids was designed by Riemer van der Vliet and adopted from literature (Bennett et al., 2021). The strategy replicates the two-plasmid expression system on pSEVA backbones with an additional *B. stearothermophilus* Mdh to assure synthetic methlotrophs SM1 and C1Saux can convert the methanol from the sMMO enzyme. In this system one plasmid contains the sMMO operon and the other plasmid contains the chaperones required for functional sMMO expression. The two plasmids are built up according to the Standard European Vector Architecture (SEVA) format. The SEVA format standardises plasmid assembly. According to the SEVA criteria the natural sequence is shortened to the smallest functional DNA sequence. Common restriction sites are removed from the sequences and gene modules are flanked by fixed, rare restriction sites (Martínez-García et al., 2020). In the cloning process for the two-plasmid system there are four interim plasmids that act as intermediates to accommodate the cloning of the large inserts. The cloning steps for the sMMO plasmid and chaperone plasmid can be viewed in figure 6&7. The interim plasmids pSEVA2610-sMMO(1-2), pSEVA2610-sMMO(3-4) and pSEVA391-chap(2-3) were achieved previously by Riemer van der Vliet. For the remaining cloning steps this leaves the plasmids pSEVA391-chap1-Mdh, pSEVA2610_sMMO_final and pSEVA391_chap_Mdh_final.

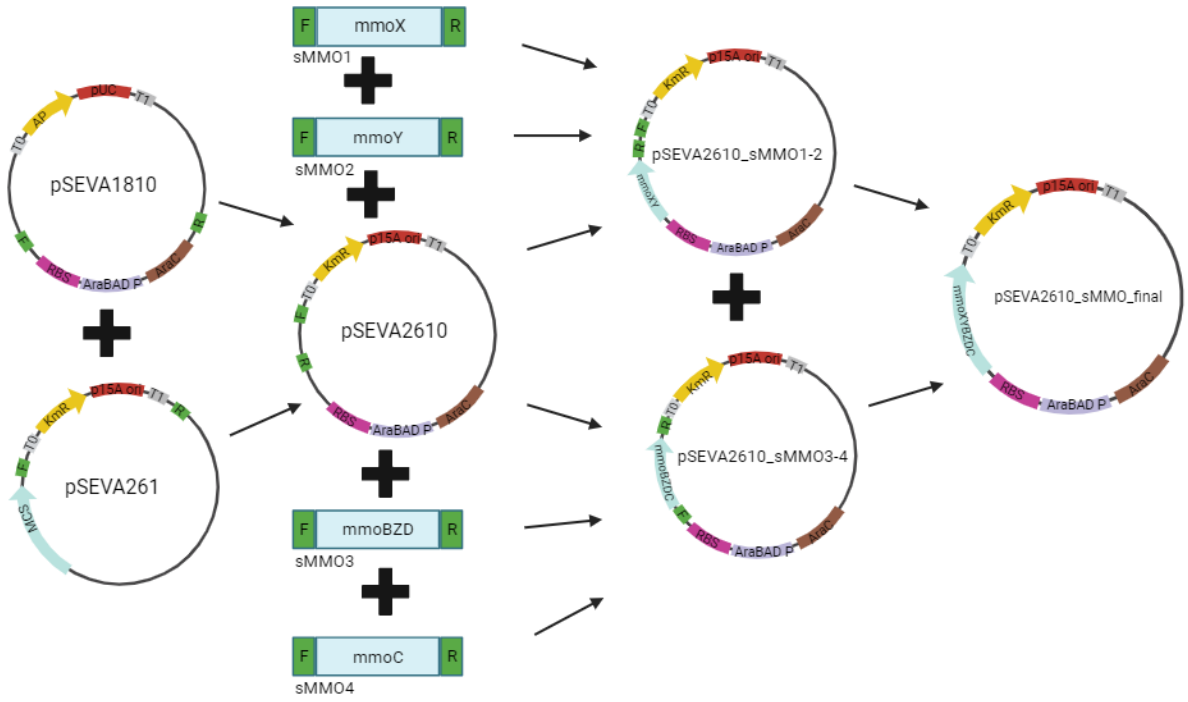

Figure 6. The cloning strategy to assemble the pSEVA2610_sMMO_final plasmid. The colours used are as follows: red is the origin of replication(ori), yellow is the antibiotic resistance, grey are terminators, green are primer binding sites, purple are promoters, pink is the ribosomal binding site (RBS), and blue is the cargo. The arrows show which parts form a product together. First pSEVA2610 is made by PCR amplifying the pSEVA261 backbone and the pSEVA1810 AraBADC promoter system that are ligated through Gibson assembly. Then intermediate plasmid pSEVA2610_sMMO1-2 is assembled from the amplified backbone of pSEVA2610, sMMO1 from the *M. capsulatus (bath) mmoX* gBlock from Integrated DNA Technologies (IDT) and sMMO2 from another IDT gBlock containing *mmoY*. The intermediate plasmid pSEVA2610_sMMO3-4 is assembled from amplified pSEVA2610 backbone, sMMO3 from a *bath mmoBZD* gBlock from IDT and sMMO4 from *Bath* gBlock containing *mmoC* from Twist Bioscience (Twist BS). The expression plasmid pSEVA2610_sMMO_final is assembled from the amplified backbone from pSEVA2610_sMMO1-2 and the amplified cargo (*mmoBZDC*) from pSEVA2610_sMMO3-4.

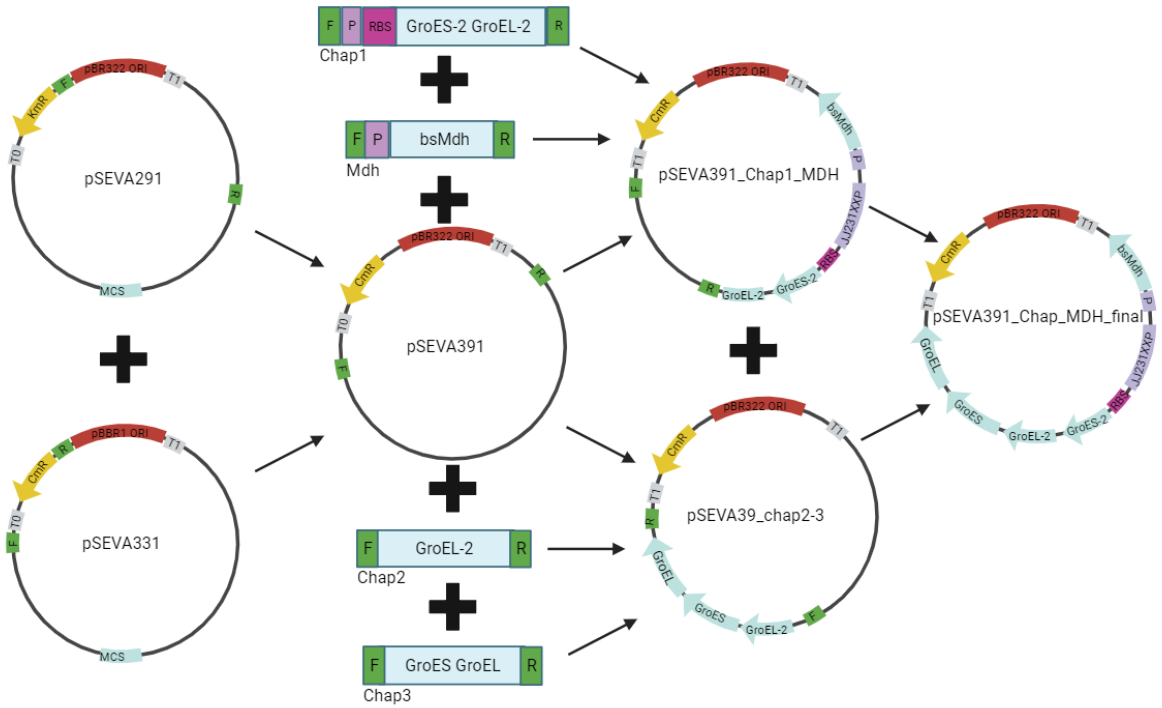

Figure 7. The cloning strategy designed to assemble the pSEVA391_Chap_MDH_final plasmid. The colours used are as follows: red is the origin of replication(ori), yellow is the antibiotic resistance, grey are terminators, green are primer binding sites, purple are promoters, pink is the ribosomal binding site (RBS), and blue is the cargo. The arrows show which parts form a product. First pSEVA391 is made by PCR amplifying the pSEVA291 backbone and the pSEVA331 chloramphenicol resistance that are ligated through Gibson assembly. Then intermediate plasmid pSEVA391_Chap1_MDH is assembled from the amplified backbone from pSEVA391, Chap1 from the *M. capsulatus (bath)* GroESL2 gBlock from Twist bioscience (Twist BS) and Mdh from the pZASSC-rbsC-bsMDH plasmid (Wenk et al., 2020). The intermediate plasmid pSEVA391_chap2-3 is assembled from amplified pSEVA391 backbone, Chap2 from the same *M. capsulatus* GroESL2 gBlock and Chap3 from *E. coli* MG1655. The expression plasmid pSEVA391_Chap_MDH_final is assembled from the amplified backbone from pSEVA391_Chap1_MDH and the amplified cargo (truncated GroEL2 and GroESL) from pSEVA391_chap2-3.

Cloning

The main method used to obtain the plasmids was amplifying fragments with primers to create matching overhangs and ligate through Gibson assembly. Plasmids pSEVA291, pSEVA331, pSEVA2610_sMMO1-2, pSEVA2610_sMMO3-4 and pSEVA391_chap2-3 were retrieved from glycerol stocks of transformed DH5α cells. The DH5α cells were transferred into 5 ml Lysogeny Broth (LB) medium (Appendix 1) with appropriate antibiotic overnight (figure 6&7). The plasmids were obtained from the cells by ZymoPURE miniprep (Zymo Research). Gene fragments of interest pSEVA291, pSEVA331, pSEVA391, Mdh, pSEV2610-sMMO(1-2) and pSEV2610-sMMO(3-4) were amplified by PCR from plasmids while Chap1 is amplified from a g-block (Table 1). The PCR mix used was Q5® High-Fidelity 2x Master Mix. The products were checked using a 1% agarose gel in TAE buffer. The agarose gel was run at 120 V for 30 minutes. The products pSEVA291, pSEVA331, pSEVA391, Mdh, Chap1, pSEV2610-sMMO(1-2) and pSEV2610-sMMO(3-4) were purified after gel excision with the Zymoclean Gel Recovery kit (Zymo Research). The PCR products pSEVA291, pSEVA331 and pSEVA391 were also purified by DpnI digesting for 1 hour at 37°C followed by PCR clean-up using the ZR-96 DNA Clean & Concentrator® kit (Zymo Research). The parts were then assembled using the NEBuilder® HiFi DNA Assembly Master Mix (NEB) using 50 ng of vector and for each insert a 2-fold molar excess. Gibson

assembly incubation was done at 50°C for 60 minutes. After assembly 5 µl of the reaction mix was transformed by heat shock into DH5α cells. Competent DH5α cells were taken from the -80°C. The reaction mix was added to the cells and the DNA was incubated with the cells while thawing on ice for 30 minutes. Heatshock transformation was done by placing the cells in a 42°C water bath for exactly 45 seconds. The cells were shortly (2 minutes) incubated on ice. Afterwards the cells were allowed to recover by adding 950 µl LB medium and incubating at 37 °C for 60 minutes. For plating, appropriate antibiotic selection plates were used on which 50 µl cell suspension was spread over half the plate, the remaining cells were spun down at 1000g for 20 minutes, aspirated, and then spread on the other half of the plate. Colony PCR (cPCR) was done on the colonies to check for successful fragment assemblies using *OneTaq* (NEB). After cPCR confirmation the plasmids were sent for sequencing to MacroGen for Sanger sequencing.

Table 1. Overview of plasmids and the parts that were used and built.

Plasmid	Fragments	Primers	Size (bp)	Part	Source
pSEVA391	pSEVA291	pBR322.F pBR322.R	2419	Backbone	SEVA
	pSEVA331	CmR-tot.F CmR-tot.R	841	CmR	SEVA
pSEVA391-chap1-Mdh	pSEVA391	RV-9.F RV-9.R	2680	Backbone	This study
	pSEVA391-chap(2-3)	RV-9.F RV-9.R	2680	Backbone	Riemer
	Chap1	RV-7.F RV-7.R	1200	Chaperone *M. capsulatus*	Twist BioScience
	Mdh	RV-8.F RV-8.R	1260	*B. stearothermophilus* Mdh	pZASSC-rbsC-bsMDH plasmid from (Wenk et al., 2020)
pSEVA391-chap-Mdh	pSEVA391-chap(2-3)	RV-22.F RV-22.R	2655	Chaperone GroESL2 *E. coli*	Riemer
	pSEVA391-chap1-Mdh	RV-23.F RV-23.R	5086	Backbone + *B. stearothermophilus* Mdh + *M. Capsulatus* chaperone GroESL	This study
pSEVA2610-sMMO	pSEV2610-sMMO(1-2)	RV-24.F RV-24.R	6470	Backbone, KmR mmoXY	Riemer
	pSEV2610-sMMO(3-4)	RV-25.F RV-25.R	2640	mmoBCDZ	Riemer

Growth assays

The *E. coli* strains SM1, C1Saux, C1Saux-Mdh and MG1655 were recovered from -80°C storage and inoculated in 10 ml (LB) medium + appropriate antibiotic (strain details in appendix 2). The cells were grown in preculture over 2 nights at 37°C at 500 rpm until an OD_{600} of 1.5. Before starting the growth assay, the cells were washed to eliminate LB media components by centrifuging at 5000g for 5 minutes, pouring the liquid off and adding 3 ml washing media, this was repeated 3 times. The media used for washing was M9 minimal medium supplemented with 20 mM glucose and 20 mM formate for C1Saux, C1Saux-Mdh and MG1655 while MOPS media supplemented with 20 mM glucose was used for SM1 (media details in appendix 1). After washing the preculture the OD_{600} was measured, between 1.1 and 1.7, and about between 4-7 µl cell suspension was added to 93-96 µl of medium in a flat bottom 96-wells plate for a final OD_{600} of 0.05 and then 50 µl mineral oil was added to prevent evaporation. The four strains were measured in triplicates and the medium conditions differed per row (table 2). OD_{600} measurements were taken every 30 minutes for 96 hours on the Elx800 platereader at 37°C shaking at 500 rpm. The platereader OD_{600} was corrected to cuvette OD_{600} by correcting the data with /0.23. The doubling time (dt) was calculated using the formulate ln2/r=dt with r being the slope. The slope was calculated with the formula $(\ln[OD_{600}2/ OD_{600}1])/(T2/T1)=r$. The time intervals showing exponential growth were chosen by plotting the $\ln OD_{600}$ against time and manually determining the linear portion. The standard deviation was calculated from corrected data (/0.23).

Table 2. Overview of the 96 wells plate layout for the growth experiment. In this experiment different strains: 1-3 MG1655, 4-6 C1Saux, 7-9 C1Saux-Mdh and 10-12 SM are grown in either M9 media (purple) or MOPS media (orange). The different media conditions that are tested for are the carbon sources containing: A glucose 20 mM, B formate 20 mM and glucose 20 mM, C formate 10 mM and glucose 20 mM, D methanol 25 mM and glucose 20 mM, E methanol 50 mM and glucose 20 mM, F methanol 100 mM and glucose 20 mM, G methanol 200 mM and glucose 20 mM, H methanol 400 mM and glucose 20 mM.

Strain	WT MG1655			C1Saux			C1Saux MDH			SM1		
Media	M9 minimal media									MOPS		
Well	1	2	3	4	5	6	7	8	9	10	11	12
A	glu 20mM	glu 20mM	glu 20mM	glu 20mM	glu 20mM	glu 20mM	glu 20mM	glu 20mM	glu 20mM	Blank	Blank	Blank
B	form 10 mM +glu 20 mM	form 10 mM +glu 20 mM	form 10 mM +glu 20 mM	form 10 mM +glu 20 mM	form 10 mM +glu 20 mM	form 10 mM +glu 20 mM	form 10 mM +glu 20 mM	form 10 mM +glu 20 mM	form 10 mM +glu 20 mM	Glu 20 mM	Glu 20 mM	Glu 20 mM
C	form 20 mM +glu 20 mM	form 20 mM +glu 20 mM	form 20 mM +glu 20 mM	form 20 mM +glu 20 mM	form 20 mM +glu 20 mM	form 20 mM +glu 20 mM	form 20 mM +glu 20 mM	form 20 mM +glu 20 mM	form 20 mM +glu 20 mM	form 20 mM+ glu 20 mM	form 20 mM+ glu 20 mM	form 20 mM+ glu 20 mM
D	meth 25 mM +glu 20 mM	meth 25 mM +glu 20 mM	meth 25 mM +glu 20 mM	meth 25 mM +glu 20 mM	meth 25 mM +glu 20 mM	meth 25 mM +glu 20 mM	meth 25 mM +glu 20 mM	meth 25 mM +glu 20 mM	meth 25 mM +glu 20 mM	meth 25 mM+ glu 20 mM	meth 25 mM+ glu 20 mM	meth 25 mM+ glu 20 mM
E	meth 50 mM +glu 20 mM	meth 50 mM +glu 20 mM	meth 50 mM +glu 20 mM	meth 50 mM +glu 20 mM	meth 50 mM +glu 20 mM	meth 50 mM +glu 20 mM	meth 50 mM +glu 20 mM	meth 50 mM +glu 20 mM	meth 50 mM +glu 20 mM	meth 50 mM +glu 20 mM	meth 50 mM +glu 20 mM	meth 50 mM +glu 20 mM
F	meth 100 mM +glu 20 mM	meth 100 mM +glu 20 mM	meth 100 mM +glu 20 mM	meth 100 mM +glu 20 mM	meth 100 mM +glu 20 mM	meth 100 mM +glu 20 mM	meth 100 mM +glu 20 mM	meth 100 mM +glu 20 mM	meth 100 mM +glu 20 mM	meth 100 mM +glu 20 mM	meth 100 mM +glu 20 mM	meth 100 mM +glu 20 mM
G	meth 200 mM +glu 20 mM	meth 200 mM +glu 20 mM	meth 200 mM +glu 20 mM	meth 200 mM +glu 20 mM	meth 200 mM +glu 20 mM	meth 200 mM +glu 20 mM	meth 200 mM +glu 20 mM	meth 200 mM +glu 20 mM	meth 200 mM +glu 20 mM	meth 200 mM +glu 20 mM	meth 200 mM +glu 20 mM	meth 200 mM +glu 20 mM
H	meth 400 mM +glu 20 mM	meth 400 mM +glu 20 mM	meth 400 mM +glu 20 mM	meth 400 mM +glu 20 mM	meth 400 mM +glu 20 mM	meth 400 mM +glu 20 mM	meth 400 mM +glu 20 mM	meth 400 mM +glu 20 mM	meth 400 mM +glu 20 mM	meth 400 mM +glu 20 mM	meth 400 mM +glu 20 mM	meth 400 mM +glu 20 mM

Results and discussion

Cloning of pSEVA391_Mdh-chap1

For the Gibson assembly of pSEVA391-Mdh-chap1 three parts are required. The approach was to amplify the pSEVA391 backbone from the successfully cloned pSEVA391-chap(2-3) (2680 bp), Mdh of *B. stearothermophilus* from a plasmid (1260 bp) and truncated GroESL of *M. capsulatus* (Chap1) from a Twist Bioscience gBlock (1200 bp). The electrophoresis gel in figure 8 confirms the correct amplification of the Mdh and chap1 fragments that can be used in the next cloning step. However, the backbone from pSEVA391 was not the expected band size. This amplification of a smaller fragment could be caused by an alternate binding site of primers. A solution was sought in changing the annealing temperature and the results in figure 9 showed multiple bands. The decrease of annealing temperature allowed for more primer binding sites resulting in more off target bands. The bands at the expected height of

2680 bp were excised from the gel and used for Gibson assembly together with the earlier obtained Mdh and chap1 fragments from figure 8. However, the transformations did not yield any colonies. The most likely reason being the unspecific amplification of the pSEVA391 backbone. Thus, another approach was taken by rebuilding the pSEVA391 plasmid. This was done by amplifying the original backbone plasmid pSEVA291 (2419 bp) and exchanging the kanamycin resistance (KmR) to chloramphenicol resistance (CmR). The chloramphenicol resistance fragment (841 bp) was obtained from amplifying pSEVA331. The following PCR analysis from figure 10 showed the desired pSEVA291 backbone fragment (2419 bp) and CmR fragment (841 bp). These fragments were further used for Gibson assembly and yielded colonies. The colonies were then checked using colony PCR (cPCR) as can be seen figure 11. The results from the cPCR show that the backbone plasmid pSEVA391 was not achieved. This can be caused by several things. There might be an issue with the used primers, unspecific binding or DNA structures that get in the way of proper amplification. There is also a slight possibility that the pSEVA291 backbone plasmid might not have the expected sequence that is shown in the plasmid map.

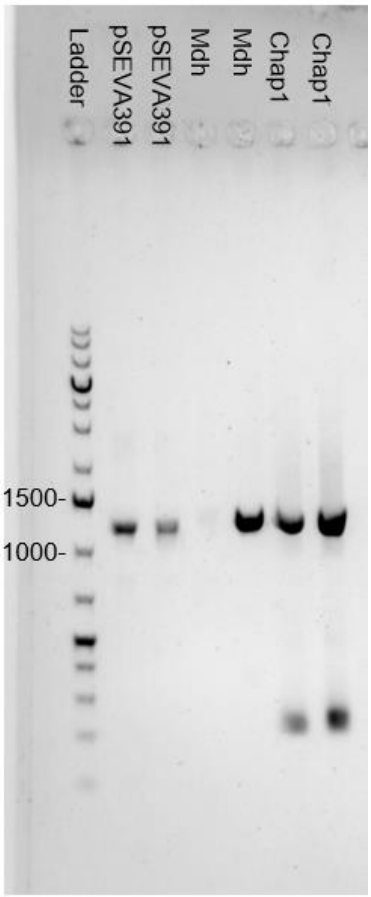

Figure 8. Electrophoresis results of pSEVA391-Mdh-chap1 parts. The gel shows that the pSEVA391 backbone bands are between the 1 Kbp and 1.5 Kbp band which is not the expected band size (2680 bp). The Mdh fragment band is between the 1 Kbp and 1.5 Kbp band as expected (1260 bp). And the chap1 fragment band is visible between 1 Kbp and 1.5 Kbp as expected (1200 bp). The ladder used is Generuler 1 Kbp plus.

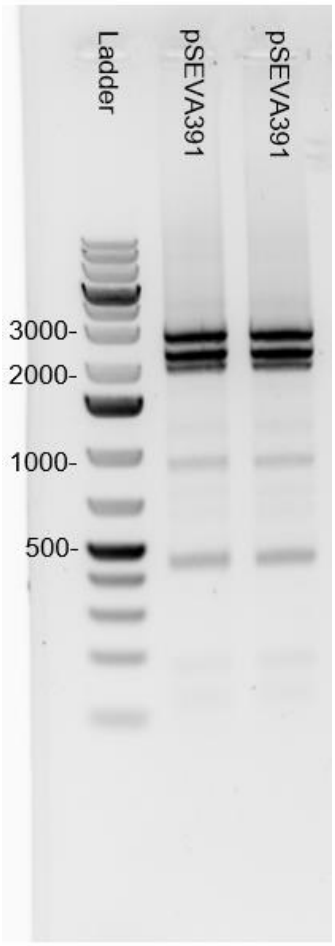

Figure 9. Electrophoresis results of pSEVA391 backbone amplification with lower annealing temperature. The gel shows multiple pSEVA391 backbone bands between the 2 Kbp and 3 Kbp band, among which is the expected height (2680 bp). The ladder used was Generuler 1 Kbp plus.

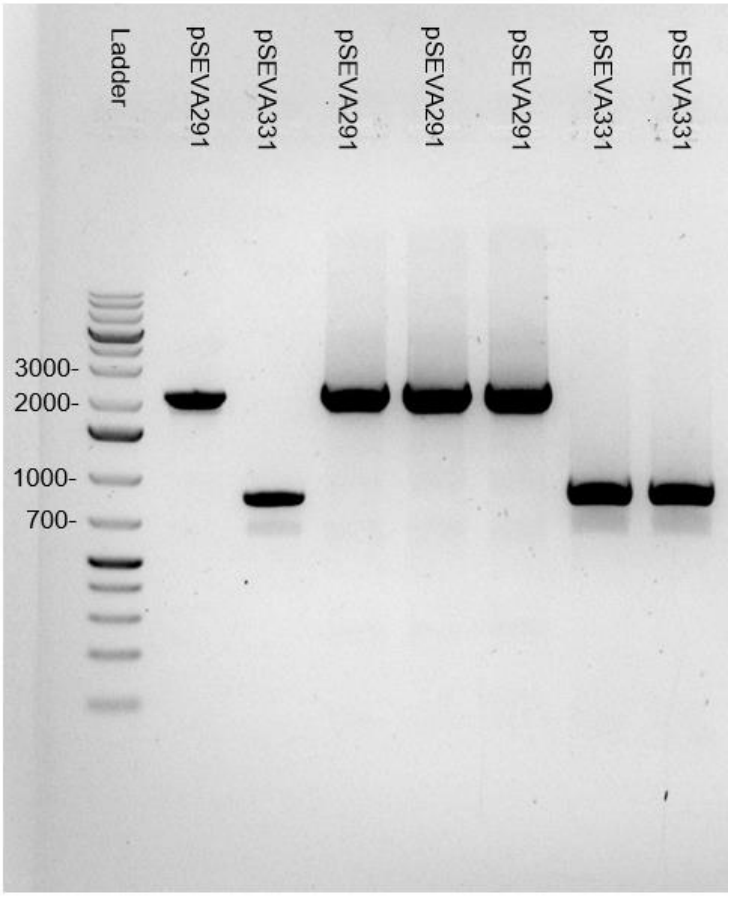

Figure 10. Electrophoresis results of pSEVA391 backbone parts. The gel shows pSEVA291 backbone bands between the 2 Kbp and 3 Kbp band which is the expected height (2419 bp). The chloramphenicol resistance bands between the 700 kb and 1 Kbp band are also at the expected height (841 bp). The ladder used was Generuler 1 Kbp plus.

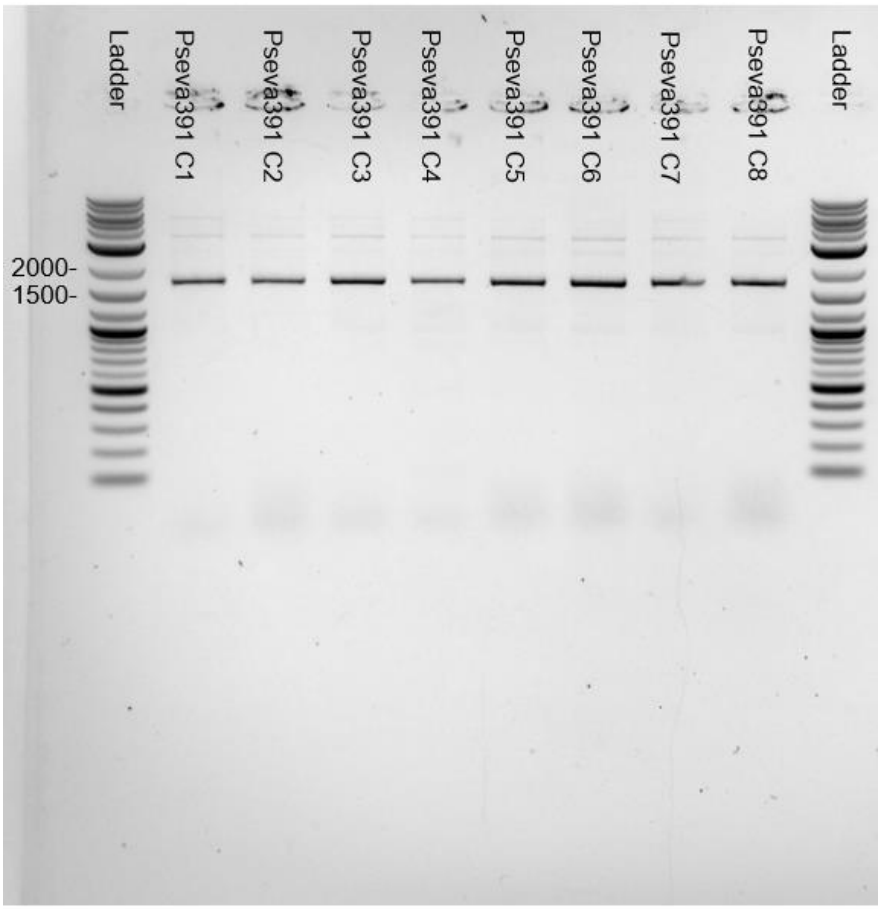

Figure 11. Electrophoresis results of pSEVA391 cPCR. The gel shows different colonies of Gibson assembled pSEVA391. The band sizes are between the 2 kbp and 1.5 kbp bands which is not the expected size (2680 bp). The ladder used was NEB 1kb plus ladder.

Cloning of pSEVA2610_sMMO

The final plasmid containing the sMMO operon was obtained from intermediate plasmids by using pSEVA2610_sMMO(1-2) as the backbone plasmid that already contains the sMMO subunits *mmoXY* subunits and using pSEVA2610_sMMO(3-4) for the subunits *mmoBZDC*. This was done by amplifying pSEVA2610_sMMO(1-2) for a fragment of 6470 bp and amplifying pSEVA2610_sMMO(3-4) for a fragment of 2640 bp. These fragments with overlapping overhangs were then ligated using a Gibson assembly reaction. The transformed plate yielded colonies of which colony 2 and 3 were sent for sanger sequencing by Macrogen. The sequencing reaction in figure 12 confirmed the presence of the gene *mmoC* from pSEVA2610_sMMO(3-4) in both samples. To gain more coverage another sequencing reaction was run using a different primer set. The sequencing results in figure 13 show an insertion in *mmoX* as indicated by the interrupted sequence in the template. The sequence found in the gap is likely a duplication of the mmoX sequence. This result confirms the presence of both pSEVA2610_sMMO(1-2) and pSEVA2610_sMMO(3-4) parts in the cloned pSEVA2610_sMMO. However, this plasmid should not be used for sMMO expression without fixing the gene of interest and sequencing the entire plasmid.

Figure 12. Sequencing results of pSEVA2610-sMMO genes of interest. The primer set used was PS1 and PS2. The genes amplified are *mmoC* and AraC regulator. The sequenced genes show no insertions or deletions or frame shifts or point mutations resulting in different amino acids.

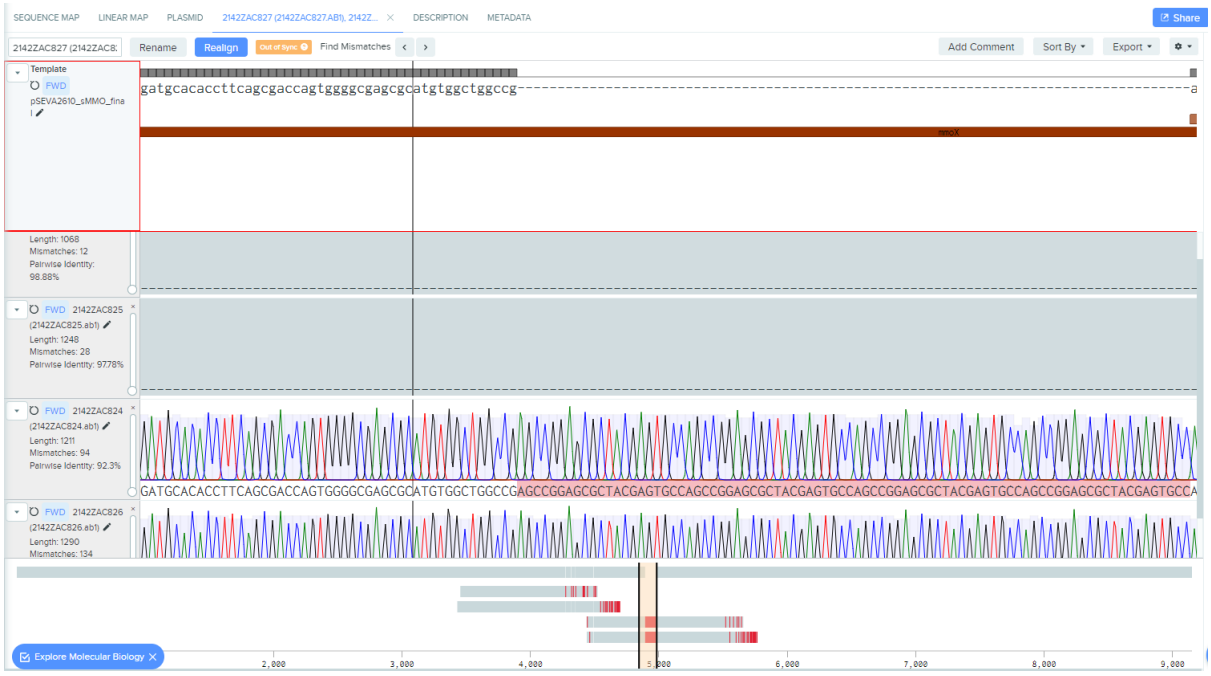

Figure 13. Sequencing results of pSEVA2610-sMMO *mmoX* gene. The primer set used was BG27809 and BG27810. The fragments amplified are in the *mmoX* gene. The sequence shows an insertion in the *mmoX* gene.

Growth experiment

To attempt synthetic methanotrophy it is important to determine a suitable synthetic methylotrophic host for the sMMO enzyme. A growth experiment was set up to determine the characteristics of the C1Saux strain and SM1 strain when cultured on different carbon sources and concentrations. The strains are cultured on either M9 or MOPS medium and carbon source concentrations comparable to literature (Chen et al., 2020; Yishai et al., 2017). The main difference between the strains is that SM1 strain is made to grow fully on

methanol as carbon source using the RuMP pathway and C1Saux is for 1-3% of its biomass dependent on formaldehyde that is metabolised using the rGly pathway. It is expected that the SM1 strain can grow on MOPS media with 400 mM methanol as its only carbon source to a maximum OD_{600} of 2 with a doubling time of 8 hours (Chen et al., 2020). The SM1 strain has a mutated glycolysis pathway from multiple rounds of adaptive laboratory evolution (ALE) which directs flux towards the RuMP pathway. The SM1 strain is expected to grow slower than wild type (WT) MG1655 *E. coli* when cultured on glucose because of the redirected flux. SM1 is not expected to grow when cultured on formate as sole carbon source because formaldehyde is used in the RuMP pathway and *E. coli* cannot efficiently reduce formate to formaldehyde. It is expected that the C1Saux strain can grow on M9 minimal media containing carbon sources of at least 10 mM glucose when supplied with 5 mM formate to an OD_{600} of 1.8 and doubling every 1.6 h (Yishai et al., 2017). The C1Saux strain cultured with just glucose as carbon source is not expected to grow because of the serine auxotrophy that can only be relieved by formate metabolism. The C1Saux is neither expected to grow when cultured on glucose and methanol as it naturally lacks a Mdh to convert methanol. To allow C1Saux metabolise methanol derived from the sMMO enzyme an C1Saux-Mdh strain was included in the experiment. The C1Saux-Mdh strain is transformed with the pZASSC-rbsC-bsMDH plasmid and allows it to use the NADH dependant Mdh of *B. stearothermophilus* (Wenk et al., 2020). It is expected that the C1Saux-Mdh strain has similar characteristics of max OD_{600} and doubling time as the C1Saux strain but with the added ability to grow on glucose with methanol substrate. The doubling time of MG1655 in minimal media and glucose is reported to be around 1 h (Thakur et al., 2010). The results of the growth experiment with only glucose as carbon source can be seen in figure 14.

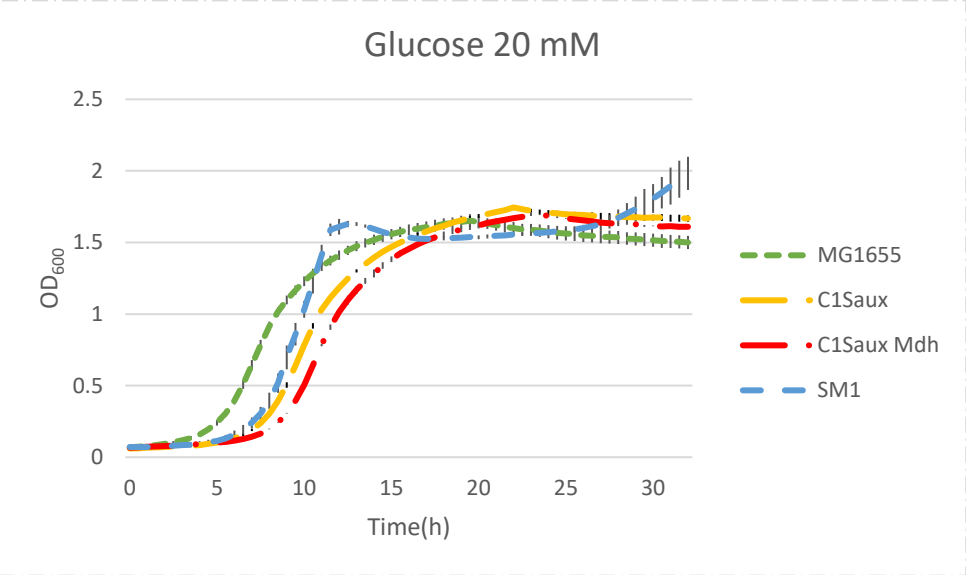

Figure 14. Growth curves of MG1655, C1Saux, C1Saux-Mdh and SM1 cultured on 20 mM glucose. The vertical error bars are calculated from technical replicates with a sample size of 3. The x axis represents time in hours and the y axis represents the OD_{600} value.

Figure 14 shows the growth curves of the strains MG1655, C1Saux and C1Saux-Mdh cultured on M9 minimal media and SM1 on MOPS media with 20 mM glucose as carbon source. All strains in this condition show growth. The WT MG1655 strain has a lag phase of 4 h, a doubling time of 2.7 h and maximum OD_{600} of 1.6. The doubling time is slower than expected and could be caused by the growing conditions in the plate reader set-up. The long lag phase can be explained from the suboptimal pre-culture that was not maintained at the log phase. The C1Saux strain has a lag phase of 6.5 h, a doubling time of 2.7 h and a

maximum OD_{600} of 1.7. The growth of the C1Saux strain in this condition is unexpected as the C1Saux strain cannot grow without serine metabolism that is not being provided. It is unlikely that the strain reacquired the deleted *serA* and *gcvTHP* gene activity. Either the media used contains formate or there is a strain present from contamination that was already able to grow on glucose as its only carbon source. Further results on the C1Saux strain should not be considered as C1Saux characteristics because of the unexpected growth in this condition. The C1Saux-Mdh strain has a lag phase of 7.5 h, a doubling time of 2.7 h and a maximum OD_{600} of 1.7. The C1Saux-Mdh strain just like the C1Saux strain is not expected to grow on only glucose as carbon source. The other platereader results of the C1Saux-Mdh strain should also not be viewed as C1Saux characteristics because of the possibilities of an unknown amount of formate in the medium or possible contamination. The SM1 strain has a lag phase of 6 h, a doubling time of 2.3 h and a maximum OD_{600} of 2.0. The SM1 doubling time is unexpected as glycolysis related genes are mutated which should result in a slower doubling time than the WT *E. coli* MG1655 strain. The faster doubling time could be caused by the overgrown preculture which could lead to a difference. Another carbon source condition tested was 20 mM formate + 20 mM glucose, a condition that should be optimal for the C1Saux strain and can be viewed in figure 15.

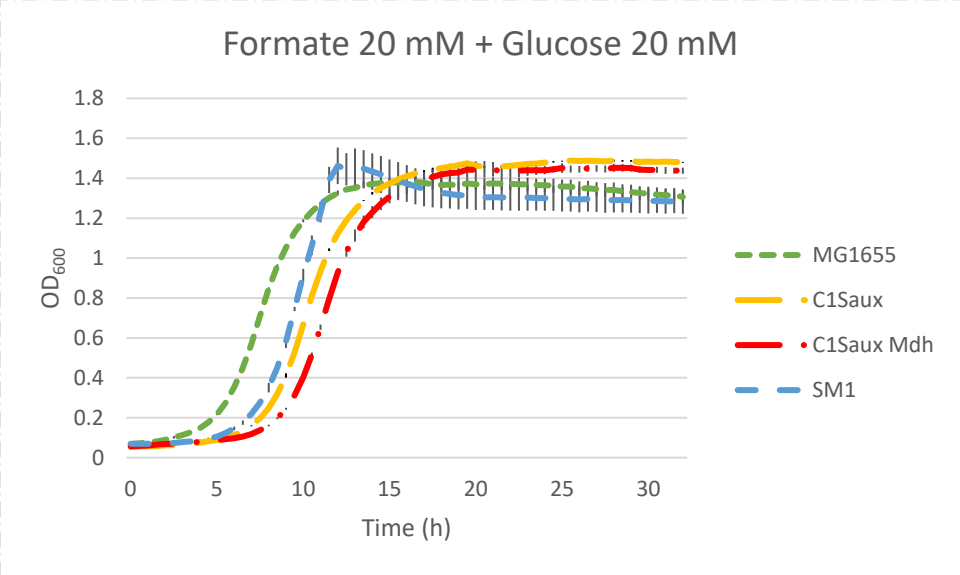

Figure 15. Growth curves of MG1655, C1Saux, C1Saux-Mdh and SM1 cultured on 20 mM glucose + 20 mM formate as carbon source. The vertical error bars are calculated from technical replicates. The x axis represents time in hours and the y axis represents the OD_{600} value.

Figure 15 shows the growth curves of the tested strains cultured on 20 mM glucose and 20 mM formate. When comparing figure 15 to figure 14 it becomes apparent that the strains MG1655, C1Saux, C1Saux-mdh and SM1 grow with a similar doubling time but with a slightly lower maximum OD_{600} in the presence of formate. Growth in this condition is expected for all strains as the media contains glucose for glycolysis in the MG1655 and SM1 strain and formate as carbon source that provides the C1Saux strains with the C1 building blocks for growth. The lower max OD_{600} might be influenced by formate toxicity. The WT MG1655 strain has a lag phase of 4 h, a doubling time of 2.7 h and maximum OD_{600} of 1.4. The C1Saux strain has a lag phase of 7 h, a doubling time of 2.7 h and a maximum OD_{600} of 1.5 The C1Saux strain is expected to grow with a doubling time of 1.6 h when grown on 10 mM glucose and supplied with 5 mM formate. However, it is already determined from figure 14 that C1Saux and C1Saux-Mdh are not showing characteristics attributable to C1Saux because of the unexpected growth seen on glucose as carbon source. The C1Saux-Mdh

strain has a lag phase of 8 h, a doubling time of 2.7 h and a maximum OD_{600} of 1.4. The SM1 strain has a lag phase of 6.5 h, a doubling time of 2.4 h and a maximum OD_{600} of 1.4. The SM1 strain is expected to grow in this condition because of the glucose present in the media. To see if there is no contamination a more informative condition would be to culture SM1 on just formate as growth on this carbon source is not expected. A carbon source for which SM1 is optimized to grow on is 400 mM methanol. In figure 16 the growth of strains is tested on 400 mM methanol + 20 mM glucose.

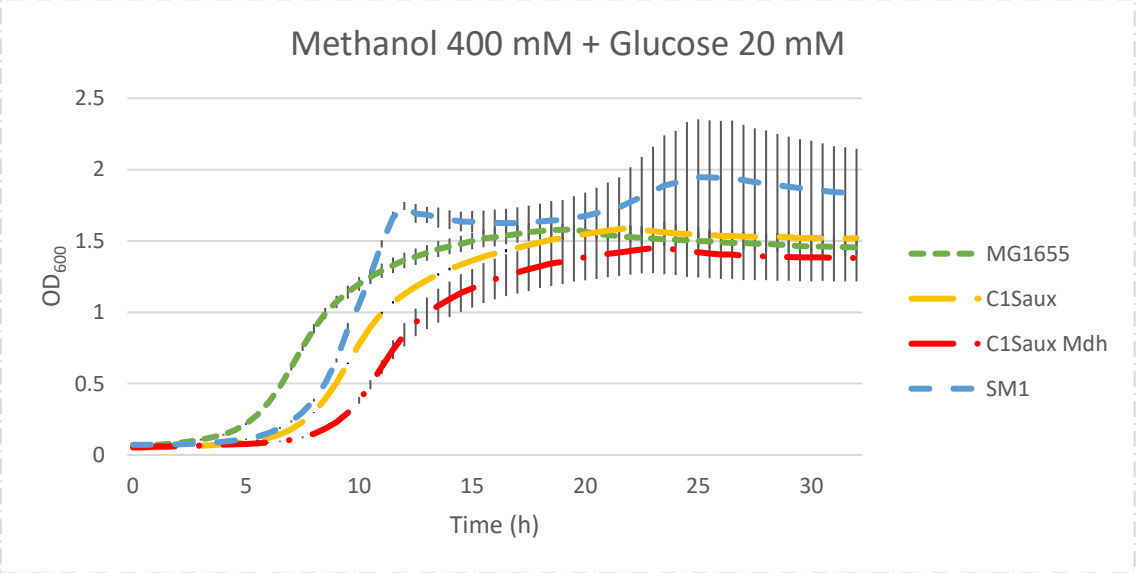

Figure 16. Growth curves of MG1655, C1Saux, C1Saux-Mdh and SM1 cultured on 20 mM glucose + 400 mM methanol as carbon source. The vertical error bars are calculated from technical replicates. The x axis represents time in hours and the y axis represents the OD_{600} value.

Figure 16 shows the growth curves of the strains cultured on 400 mM methanol and 20 mM glucose. The figure shows growth for every strain in this media condition. The growth of the strains MG1655, C1Saux-mdh and SM1 are expected with these carbon sources. C1Saux however has no means to generate serine from methanol and should not be able to grow. The WT MG1655 strain has a lag phase of 4.5 h, a doubling time of 2.6 h and maximum OD_{600} of 1.6. These growth curves are very similar to growth on just 20 mM glucose. This growth is expected as *E. coli* can tolerate up to 1 M methanol and 400 mM is well below this threshold (Bennett et al., 2021). The C1Saux strain has a lag phase of 7 h, a doubling time of 2.7 h and a maximum OD_{600} of 1.6. This strain is not expected to grow in this condition as it does not have a Mdh to metabolise methanol into formate and serine. The C1Saux-Mdh strain has a lag phase of 8 h, a doubling time of 2.9 h and a maximum OD_{600} of 1.4. Growth of this strain is expected but it is still unclear whether there is a contamination or additional formate in the M9 minimal media stock resulting in the observed growth. The SM1 strain has a lag phase of 6 h, a doubling time of 2.2 h and a maximum OD_{600} of 2.0. Growth in this condition is expected since glycolysis in this strain is mutated to have flux run through the RuMP pathway. This strain is reported capable of growing on only methanol as carbon source. Adding a test condition where SM1 is cultured in just methanol would be more informative for the purpose of finding a synthetic methylotroph. Doubling time when grown on only methanol as carbon source should be 8 h. In figure 17 the C1Saux strain growth on different tested carbon sources are being shown in a single graph to see if there any trends.

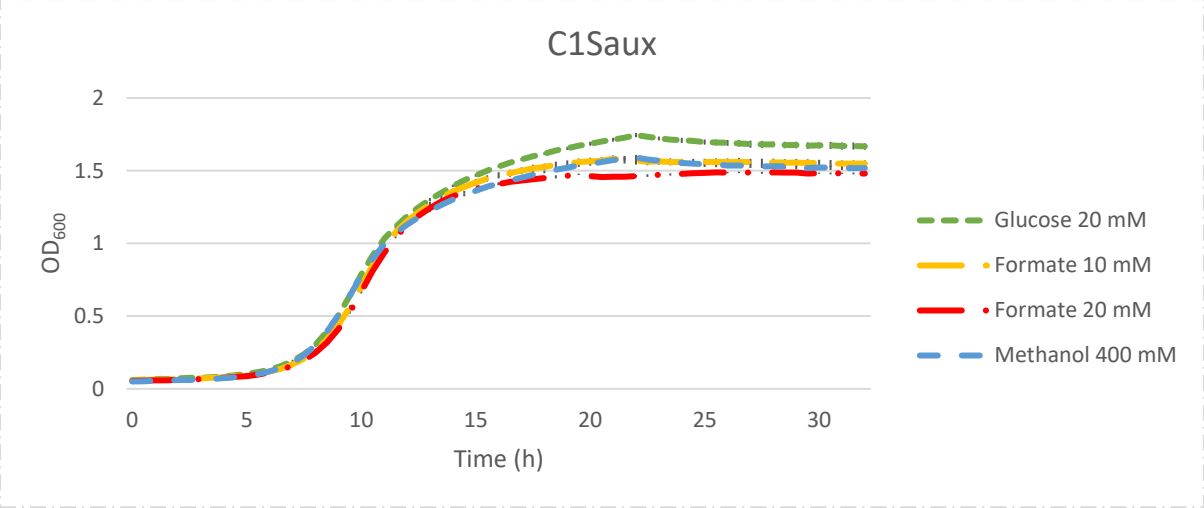

Figure 17. Growth curves of C1Saux cultured on 20 mM glucose with different added carbon sources. The different carbon sources are as follows: green just glucose, yellow 10 mM formate + 20 mM glucose, red 20 mM formate + 20 mM glucose and blue 400 mM methanol + 20 mM glucose. The vertical error bars are calculated from technical replicates. The x axis represents time in hours and the y axis represents the OD_{600} value.

Figure 17 shows C1Saux cultured with different carbon sources. The carbon sources are as follows: 20 mM glucose, 10 mM formate + 20 mM glucose, 20 mM formate + 20 mM glucose and 400 mM methanol + 20 mM glucose. The growth experiment shows that the tested strain grows in every tested carbon source condition. Growth is only expected with 10 mM and 20 mM formate + 20 mM glucose because of the C1Saux dependence on formate metabolism to generate serine and its metabolites necessary for growth. And when C1Saux is grown on formaldehyde and glucose to reach a doubling time of 1.6 h. The results however do not match the expectations. The lag time seen in all conditions is between 6.5-7 h with a doubling time of consistently 2.7 h and a max OD_{600} measured between 1.5 and 1.7. What can be seen from the growth curves are similar lag times and doubling times. There is a slight difference in max OD_{600} that suggests a growth inhibiting effect from the additional carbon sources formate and methanol. When comparing the C1Saux doubling time to the WT *E. coli* strain MG1655 in figure 14 they are both 2.7 h. However, it remains unclear whether there is formate present in the media or a contamination from the preculture. The SM1 strain results have also been compiled to see if there is a correlation between carbon source concentration and growth and these results can be viewed in figure 18.

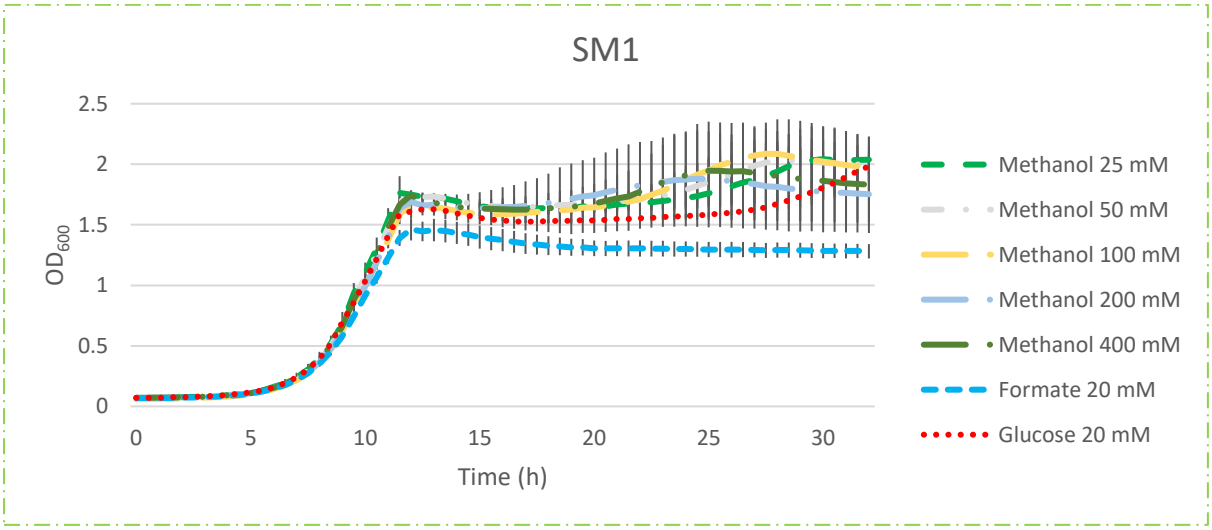

Figure 18. Growth curves of the SM1 strain cultured on 20 mM glucose with different added carbon sources. The vertical error bars are calculated from technical replicates. The x axis represents time in hours and the y axis represents the OD_{600} value.

Figure 18 shows SM1 cultured on 20 mM glucose and different added carbon sources. The carbon sources being compared are: 25 mM methanol + 20 mM glucose, 50 mM methanol + 20 mM glucose, 100 mM methanol + 20 mM glucose, 200 mM methanol + 20 mM glucose, 400 mM methanol + 20 mM glucose, 20 mM formate + 20 mM glucose and 20 mM glucose. The SM1 strain shows growth on all conditions as is expected with glucose and a glycolytic pathway that has mutated flux towards to RuMP pathway but remains functional. The lag time observed is between 6 and 6.5 h, the doubling time is between 2.2 and 2.4 h, and the max OD_{600} is between 1.5 and 2.1. The compared results show a difference mainly when cultured with 20 mM formate + 20 mM glucose where there seems to be an inhibitory effect from formate. There is no observable difference between methane concentrations impacting growth.

Together the growth experiment results were not convincing in confirming either the SM1 or C1Saux strain as hosts able to grow on the methanol generated by sMMO when cultured on methane as carbon source in the case of SM1 or methane + glucose in the case of C1Saux transformed with *B. stearothermophilus* Mdh. From the results it is strongly suggested that the pre-culture can be improved by maintaining log phase culture. The unexpected growth from C1Saux on 20 mM glucose and 400 mM methane + glucose could be caused by either a contamination in the preculture, as all C1Saux and C1Saux-Mdh show similar growth, or formate being present in the M9 stock media that generates serine for the auxotrophy. The SM1 strain is reported to grow on just methanol with optimal growth on 400 mM methanol. A more informative carbon source condition to cultivate the SM1 strain in would be 25 mM methanol, 50 mM methanol, 100 mM methanol, 200 mM methanol, 400 mM methanol, 20 mM formate and 20 mM glucose. When cultured on just glucose similar growth is expected as seen from these results. When cultured on just formate no growth is expected, that could give some more indication on whether there is a contamination from preculture or not. A repeat experiment with just one carbon source for the SM1 strain per culture condition and new M9 minimal stock media for C1Saux with a logarithmic dilution for formate would give more insight into choosing a suitable synthetic methanotroph. The expected trends in the result from the new culturing conditions would be to see growth rates slowing down in response to lower methanol/carbon source concentrations and the maximum OD_{600} to be lower at limiting carbon source concentrations. The following section will go into the next steps that can be made in establishing a synthetic methanotrophy by *E. coli* for the Cattlelyst biofilter.

Recommendations

The goal during this thesis is to set up a proof-of-concept synthetic methanotroph for the innovative Cattlelyst biofilter that is designed to convert both methane and ammonia. The approach taken to make this synthetic methanotroph was to build on the landmark achievements that are synthetic methylotrophs and expand their substrate spectrum to methane. Multiple of these synthetic methylotrophs are made in *E. coli* strains through extensive metabolic engineering to use methanol or formate as substrate. In theory adding a methane monooxygenase enzyme that converts methane to methanol and an additional methanol dehydrogenase should allow the synthetic methylotrophs to metabolise and grow on methane as substrate. Bennett et al. (2021) developed a sMMO expression system and introduced this in a synthetic methylotrophic *E. coli* strain (Δ*frmA*Δ*pgi* + pUD11) (Bennett et al., 2018). When this strain is grown on methane or methanol and glucose as co-substrate it produces acetone. However, for the Cattlelyst biofilter the preferred synthetic methylotroph is

optimized for methane uptake and cell maintenance in the limiting biofilter conditions, which differs from industrial scale chemical production since the gas concentrations in cattle stable are at low percentage (v/v) and fluctuating over the day (Wu, 2016). Therefore, the intent is to use the sMMO expression system from the Bennett et al. (2021) in a more suitable methylotroph such as the C1Saux strain and the SM1 strain (Yishai et al., 2017;Chen et al., 2020). The SM1 strain is based on the RuMP pathway and through metabolic engineering, rational design and adaptive laboratory evolution able to grow on methanol as sole carbon source. This would be beneficial for the biofilter since no additional carbon source would be needed to maintain the biofilter which reduces operation costs. Type I methanotrophs which are known to utilise low methane ppm streams use the RuMP pathway. The C1Saux strain converts formate into serine using the reductive glycine pathway. This formate consumption relieves the serine auxotrophy and serine metabolism makes up 1-3% of the cells' biomass. Introducing Mdh in conjunction with sMMO via plasmids should allow the C1Saux strain to metabolize methane into methanol and then further into formaldehyde that native formaldehyde dehydrogenases convert into formate. The C1Saux strain requires less methane for the cellular metabolism and would be ideal in the scenario where the low methane concentrations are too low to maintain a dense biofilm in the biofilter. The C1Saux also has the added benefit that it can act as a lower demand sensor strain in response to lower activity of the sMMO enzyme than SM1 strain can.

During the timespan of the thesis, it was not possible to test the biobricks for sMMO expression and a suitable synthetic methanotroph could not be established. The thesis resulted in a completed plasmid for the sMMO subunits as seen in the sequencing results with a duplication in *mmoX* gene. A completed chaperone expression vector for GroESL from *E. coli,* GroESL2 from *M. capsulatus* (bath) and methanol dehydrogenase from *B. stearothermophilus* could not be completed. The growth experiments did not show methylotrophic doubling times or optic densities (OD_{600}) as expected from literature. Both the chaperone plasmid and synthetic methylotroph parts for the synthetic methanotroph could not be validated due to time constrains. The next section will describe several experiments that can be done if more time and resources were available to achieve the chaperone plasmid for the sMMO expression system and to obtain a suitable synthetic methylotroph for the Cattlelyst biofilter.

sMMO expression plasmid

The biobricks for the sMMO units and the chaperones GroESL and GroESL2 designed by Riemer van der Vliet for a dual plasmid set-up are similar to the expressions system from Bennett et al. (2021) and should be used when pursuing the heterologous expression of sMMO in *E. coli*. The biobricks in their current state are one complete plasmid containing the sMMO subunits called pSEVA2610-sMMO, a plasmid containing the *E. coli* GroESL called pSEVA391-chap-(2-3), and a gBlock containing the *M. capsulatus* GroESL2 sequence. The original strategy was to use Gibson assembly to make plasmid pSEVA391-chap(1)-Mdh using PCR amplified backbone pSEVA391 with primer pair RV-9.F/R, chaperones GroESL2 with primer pair RV7.F/R and BsMdh with primer pair RV-8.F/R. The final plasmid pSEVA391-chap-Mdh can then be Gibson assembled by opening pSEVA391-chap(1)-Mdh with primer pair RV.23F/R and adding the *E. coli* GroESL chaperones fragment by PCR amplifying plasmid pSEVA391-chap-(2-3) with primer pair RV.22F/R.

However, due to improper amplification of the pSEVA391 backbone that is supposed to give a 2680 bp fragment size only halve the fragment size of ~1.3kb was obtained, suggesting unspecific/off-target amplification of the fragment. The pSEVA391 backbone was PCR amplified from pSEVA391-chap-(2-3) using primers RV.7-F/R and from reassembled pSEVA291 and pSEVA331. However, both these strategies did not produce the expected

PCR fragment of the pSEVA391 backbone. A temperature gradient was used for the annealing temperature and more fragments were amplified. One of the fragments was of the expected size and excised from gel. A Gibson reaction was attempted with the excised pSEVA391 PCR product, but this did not yield any viable colonies.

A way to approach the problem of having unspecific PCR products is by using different primers that bind more specifically. A different cloning strategy that can be attempted is by amplifying pSEVA391-chap-(2-3) with primers that open the plasmid at the location of RV.9-R, before the *E. coli* GroESL sequence and have similar overhangs to RV.8-R and RV.7-F to enable the J231XX promotor before the *M. capsulatus* GroESL to express all chaperones. If the Gibson assembly is not able to assemble the parts, then different cloning strategies such as restriction ligation can be used. If the pSEVA391 backbone is not able to be amplified a different backbone could be used for the chaperones in the sMMO plasmid expression system. This backbone would be required to be another *E. coli* ori plasmid with a similar medium copy number plasmid (CloDF13 ORI) and avoiding kanamycin resistance as not to have the same antibiotic resistance as plasmid pSEVA2610.

In the Bennett et al. (2021) paper directed lab evolution was used on sMMO to improve its activity. They did this by mutating one amino acid in the sequence to one of the other 19 amino acids. In total ~32,000 clones were sampled and 5 mutations improved methane oxidation. It is unclear how these mutations improved methane oxidation but one of the hypotheses is that the solubility improved. For the Cattlelyst biofilter a sMMO with high methane affinity is preferred. A similar mutation study could be done to improve methane conversion on methane levels found in the Cattlelyst biofilter to maximise the elimination capacity of the biofilter. The enzymes that perform better at low methane concentrations will need a higher affinity to bind the substrate and thus have a lower methane turnover rate. Ideally, a synthetic methylotroph that can express higher density of sMMO will alleviate the lower turnover rate and still allow for high elimination capacity of methane airstreams with a lower methane percentage (v/v). Improving methane affinity can also improve the methanotrophic activity by reducing unspecific ammonia binding that inhibits methane conversion with nitrification (Novikov & Stepanov, 2002).

Synthetic methylotroph

In this thesis the growth experiment measured C1Saux and SM1 growth on different carbon source concentrations comparable to conditions reported in literature (Chen et al., 2020; Yishai et al., 2017). The results however did not show methylotrophic growth. A growth experiment was set up by measuring OD_{600} at 37°C in a 96-wells plate over a 96-hour period. The medium conditions tested were glucose 20 mM, glucose 20 mM + methanol 400/200/100/50/25 mM and glucose 20 mM + formate 20/10 mM in the respective MOPS/M9 minimal media for each strain. The expectation for C1Saux is to only grow on the glucose + formate media conditions with a doubling time of 1.6 hours (Yishai et al., 2017). The expectations for the C1Saux strain transformed with pZASSC-rbsC-bsMDH plasmid (Wenk et al., 2020) is to grow on the glucose + formate conditions with a doubling time of 1.6 hours and when cultured on glucose + methanol conditions to possibly see slower doubling time limited by the efficiency of Mdh from the pZASSC-rbsC-bsMDH plasmid. The expectation for the SM1 strain was to show optimal growth on 400 mM methanol with a doubling time of 8 hours to a max OD_{600} of 2 and to see carbon dependant growth on lower conditions (Chen et al., 2020). All samples except for the blank condition showed similar growth with doubling times between 2-3 hours and with a maximum optic density OD_{600} of 2.1. This growth is as expected as the glycolytic flux is mutated toward the RuMP pathway but remains intact. The different timepoints in reaching the max OD_{600} between wildtype and the SM1 strain could stem from the preculture error, this seems to be the case when looking at overlapping

growth curves the strains. The experiment should be repeated starting from a better starting cell suspension that is preferably between an OD_{600} of 0.4-0.8 so each strain can grow from the log phase. When repeating the experiment, it is important to avoid contaminations when handling multiple samples. A fresh stock of M9 minimal media is also recommended to avoid unknown concentrations of carbon sources being present in media/the experiment.

The growth conditions were not optimal to determine the strain characteristics. All carbon source conditions contained glucose, which for the C1Saux strain is a requirement since it cannot grow solely on formate. However, the SM1 strain was built using a xylose auxotrophy strategy, requiring xylose and methanol for glycolysis. The glucose metabolism is mutated through multiple rounds of adaptive laboratory evolution. The SM1 strain with glycolysis flux redirected through the RuMP pathway is expected to grow faster when cultured on glucose than on methanol, but at a slower doubling time than WT *E. coli* strain. If the experiment would be repeated it is important to have a condition with SM1 growing on MOPS media with just 400 mM methanol as carbon source to check if the reported doubling time and OD_{600} can be achieved in the replicated set-up.

In a repeat experiment it would still be interesting to see the growth of SM1 and C1Saux on formate and methanol with a logarithmic dilution to see the characteristics such as doubling time, maximum optic density with restricted carbon source availability and possibly the death phase. The microplate-reader set-up of the growth experiment is also important. The ELx800 used could have suboptimal temperature control resulting in the observed slower growth rate. This can be especially problematic with longer running experiments and getting the SM1 strain with already lengthy doubling time to grow.

The follow-up experiment after C1Saux and SM1 show comparable growth as reported in literature would be to look at physiologically relevant conditions in a cow stable biofilter. Cow stables are optimally kept between 4 °C to 16 °C (Johnson, 1965). Under Henry's law a 1% methane airstream results in a dissolved methane concentration of ~20 µM at 15 °C and 1 atm mM dissolved methane (Cookney et al., 2016). For the biofilter application on low (v/v) methane concentrations it is interesting if C1Saux and SM1 can sustain biomass under these conditions. The follow up experiment would have to be incubated at 15 °C and started at an OD_{600} of 0.1-0.3 to check whether cells can sustain biomass or will die off.

After a suitable synthetic methylotroph is obtained it can be made more suitable as the chassis organism for the synthetic methanotroph. At this stage the strain engineering required for the Cattlelyst biofilter to have a co-culture that is amino acid/carbon dependant, and the safety switches can be tested on a reduced carbon substrate (e.g. methanol or formate). These modules can be tested individually in proof-of-concept experiments as all the strain engineering is novel. A synthetic methylotroph that is optimized for efficient growth on methanol would be optimal for the biofilter. The fastest growing isolated methanotroph has a specific growth rate of 0.40 h^{-1} on 80% air and 20% methane airstream supplied in chemostat. This methanotroph belongs to gammaproteobacterial genera and these bacteria use the RuMP pathway to metabolise methane (Kim et al., 2018). This rapid growth on methane highlights the potential of the RuMP pathway to efficiently metabolise methane into biomass.

Investigating how the metabolic pathway is optimized and regulated would be interesting for the balancing of enzymes in the synthetic pathway. The end goal is to make a synthetic methanotroph for the Cattlelyst biofilter. The synthetic methylotroph can be optimised using culturing conditions which simulate growth on carbon source levels found in the biofilter. One of the ways this can be done is through adaptive laboratory evolution on growth limiting conditions by increasingly lowering methanol concentrations and selecting for clones with

high optic density/growth rate. Taking these steps sets up a biofilter specific synthetic methylotroph.

Synthetic methanotroph

When both the sMMO expression plasmids are achieved and the growth of a suitable synthetic methylotroph are characterized on different substrate concentrations a synthetic methanotroph can be set-up quite straight forwardly. Expressing the sMMO enzyme in a suitable synthetic methylotroph such as SM1 or in C1Saux in conjunction with Mdh in theory completes the metabolic pathway required to use methane as a carbon source and facilitate growth. The first step would be to transform the methylotrophic strain. Clones can be selected for with the two antibiotic resistance genes found in the plasmids. Colony PCR can then confirm the presence of the plasmids. These transformed strains can be used as sensors to measure the conversion rate of methane by sMMO. A strain like SM1 that has a doubling time of 8 hours on 400mM methanol would most likely have a longer doubling time (Chen et al., 2020). Achieving such high methanol conversion from methane would be very difficult given the low water solubility of 1.237 mM at standard conditions (20°C 1 atm) (Guerrero-Cruz et al., 2021). The C1Saux strain has a doubling time of 1.6 hours when grown on 10 mM glucose and 5 mM formate (Yishai et al., 2017). This strain will likely show retarded growth because of the limited availability of formate as metabolite from methane. Without formate no serine can be produced, and cell growth is not possible. However, if growth is shown then the sMMO expression system produced functional sMMO enzyme and a synthetic methanotroph would be achieved. If no growth is shown further analysis such as western blotting and checking for methane consumption with gas chromatography can be done.

The growth of an *E. coli* strain on methane would be a major milestone and allow for further optimization for biofilter use. For the SM1 strain redox balancing would be recommended to improve growth. The SM1 strain has Gapdh downregulated and mutated frmA fdoG that are involved in NADH production. sMMO is NADH dependent enzyme that can regenerate the NAD+ required for Mdh activity (Gregory et al., 2022). Thus, restoring some of these NADH production mechanisms might be beneficial for growth. When the C1Saux strain is transformed with both sMMO and BsMdh redox balancing likely won't be needed since NAD+ and NADH are regenerated in the pathway and the sugar metabolism can regenerate other co-factors. Growth on low methane conditions can further be improved upon by nutrient restrictive adaptive laboratory evolution and selecting for growth that might help with the regulation/balancing of enzymes in biofilter conditions.

Cow stables are often not closed off and have a methane concentration varying over the day and with temperature (van der Zaag et al., 2014). Ruminant gas excretion content is up to ~25% methane. Per day a single cow emits roughly 1000-1300L methane. And the yearly emission of methane is 112 kg per cow (Nowakowicz-Debek et al., 2020). The methane concentration in a cow stable is roughly 40.9 mmol m^{-3}=670 µg/l=670 ppm=0.67% (Wu, 2016). The hood system that collects gases for the biofilter concentrates the emitted methane. The ventilation rate is at least 5 times smaller leading to a 5 times higher methane concentration in the biofilter. Adaptive laboratory evolution experiment should aim to culture towards these dissolved methane levels of ~60 µM at 15 °C and 1 atm (Cookney et al., 2016). Under these restricted nutrient conditions, survival and high cell density on a low methane stream are the most important qualities. Therefore, a chemostat setup is recommended. The goal of the culture is to reach an equilibrium of cell growth and cell death in biofilter conditions. The Monod equation should be equal to 0 net growth rate. If this net growth of 0 can be achieved on such low methane concentrations, then a synthetic

methanotroph is made that can survive the biofilter conditions for a prolonged time resulting in consistent methane elimination capability.

Future perspectives and limitations

Synthetic methanotrophy

Synthetic methylotrophy as a field, has made significant advances in synthetic biology, metabolic engineering and the understanding of natural methylotrophy. Synthetic methylotrophy offers a biological method to use reduced one-carbon compounds as energy or carbon source to produce value added products. Reduced one-carbon compounds as a substrate are renewable and can be produced carbon neutrally, sustainably and without competing with food sources. Synthetic methanotrophy as a subfield of synthetic methylotrophy adds the ability to convert high methane concentrations into value added products and low methane concentrations into a carbon source to maintain biofilter biomass using methane monooxygenases. Fundamental advances have been made in understanding how methane monooxygenases function. However, there are still questions, the answers of which are important for improving methanotrophy. Particulate MMO is interesting for biofilter applications because of the higher affinity to methane and allowing some methanotrophs to grow on 10-100 ppm methane (Baani & Liesack, 2008). Particulate MMO has been expressed by placing the catalytic domains on an apoferritin scaffold thus making the protein soluble and able to be expressed without a membrane (Kim et al., 2019). This particulate methane monooxygenase allowed for *ex vivo* methane conversion when supplied with duroquinol as electron donor. Duroquinol is not naturally found in methanotroph and *In vivo* results have not be shown. pMMO electron donors can be further investigated for *in vivo* application as this could open the possibility for cellular growth of synthetic methanotrophs on very low methane concentrations. Soluble MMO is more interesting for industrial purposes as the turnover rate of the enzyme is much higher than pMMO (Sirajuddin & Rosenzweig, 2015). sMMO has been functionally expressed in *E. coli* hosts by Bennett et al. (2021). This study shows that the enzyme can be heterologous expressed, isolated and improved upon. Bennett et al. (2021) did this with a mutant library for sMMO changing the amino acids one by one resulting in 5 amino acid optimizations most likely related to solubility. Such strategies together with modelling and ALE can give information on how the sMMO enzyme functions and can be optimized for different conditions. However, there's a limit to how much a synthetic methanotroph can be reasonably optimized for methane consumption. Natural methanotrophs can sense methanol and their metabolism adapts to methane concentrations (Jakobsen et al., 2006). Gene regulation in response to biofilter methane airflow conditions is very hard to achieve in synthetic methylotrophs as hundreds of genes are involved in regulating the cellular response to carbon source availability (Gregory et al., 2022). There's also a biological limit on how much extra protein a synthetic host can express. A proteomics study found that the N-MDH expression made up 40% of the protein content (Keller et al., 2022). This level of expression is hypothesized to be a burden to the strains resulting in limited growth. The main role of synthetic methanotrophs in the future will likely be in gathering knowledge to improve natural atmospheric methanotrophs through genetic editing for when their genetic tool kits become available (Sanford & Woolston, 2022). For a methane biofilter the main requirement of the methanotroph will be the maintenance of a high cell density on low methane concentrations. For a higher elimination efficiency, the methane airflow concentrations are more vital to improve than optimizing the ability of a synthetic methanotroph to convert methanol efficiently (Drinkwaard, 2021).

Methane biofilters

Most anthropogenic methane emissions are below the ignition threshold, for 55% of methane emissions a biofilter could be a more effective solution. For the use of specific cultures in biofilters a synthetic methylotroph is interesting because these methylotrophs can be engineered for the specific conditions of the biofilter environment. Synthetic methanotroph cultures also give a more measurable output since there is only one organism responsible for eliminating methane. Synthetic biofilters are currently very difficult to implement due to regulatory limitations on GMOs, safety concerns on GMOs, metabolic engineering requirements and implementation costs. According to biofilter modelling the biggest bottleneck for a methane biofilter lays in the methane transfer into the biofilter (Drinkwaard, 2021). The hood system is able to increase the methane concentrations 5-fold. However, according to expert opinion current biofilter systems need to be improved 20-fold upon in order to be economically viable. More technical innovations in biofilter design and improvement on methane availability for the biofilter are needed before a methane biofilter can be considered for implementation. A promising technology are hydrocarbon ladder polymers, membranes that are able to separate gases, including methane (Lai et al., 2022). If methane biofilters can be implemented it would be a powerful tool for efficiently and sustainably tackling complex problems such as low concentration methane emissions without the need of expensive catalysts, energy intensive processes or harsh chemicals (La et al., 2018).

Conclusion

This study investigated a method to establish a proof of concept synthetic methanotroph for the Cattlelyst biofilter. The hypothesis is that a synthetic methanotroph can be made by using established synthetic methylotrophs SM1 and C1Saux and having them heterologously express sMMO by introducing sMMO subunits (*mmoXYBZCD)*, cognate chaperones GroESL2 from *M. capsulatus* and overexpression of native chaperones GroESL from *E. coli* using a dual plasmid system. During the project the sMMO subunits plasmid was achieved with a duplication in the *mmoX* gene. However the chaperone plasmid and synthetic methylotrophic growth are not achieved and the hypothesis remains untested. The hypothesis cannot be confirmed or rejected. However, a synthetic methanotroph for biofilter application is still a goal worth pursuing to enable the advancements of methanotroph based technology. The impact of biofilter design advancements such as packing material (33%), hood system (5x), pure cultures (unknown) and hydrocarbon ladder polymers (unknown) could push methane biofilter to the 20-fold improvement needed to be economically viable.

Acknowledgements

During this thesis I struggled with burn-out, severe sleep deprivation and depression. Getting a thesis done while struggling with basic self-care has been one of the greatest challenges of my live. During this thesis I learned how to get tasks done on very limited resources and recover my mental health. This thesis would not have been possible without the support of numerous people. Many props to Eric for being able to supervise a thesis with an irregular schedule and being able to set realistic milestones in a changing project. You have taught me that a practical mindset can move mountains. I want to thank Nico for his guidance on handling life and giving insights into the field of reduced C1 metabolism. Every meeting we have had I left more inspired than before. I want to thank my therapists, psychologists and psychiatrists Marieke, Shanta, Paul, Simone, Pauline, Nico, Marlies, and Jenneke for their expertise and helping me through my distress. Thanks to their mental health care I have come to a better understanding on my unhealthy emotional patterns and now have access to a healthy approach. I want to thank my housemates Deli, Mika, Lenka, Smara and Aude for their gentleness and patience when dealing with me. Coming back to such a lively home was the best comfort I could have wish for. I want to thank my iGEM teammates Jenny, Riemer, Sanne, Deli, Marta, Thomas, Sophie, Sophieke, and Anemoon for the unique experiences and togetherness. Together we have explored many frontiers, and I am glad to have with such determined people. A special thank you to Riemer for exploring synthetic methanotrophy with me and setting up the GC experiment with Miguel Paredes Barrada to show negative preliminary results on the pMMO-mimetic *in vivo* and *in vitro* activity. I want to thank my close friends Gerben and Florian for making me able to laugh at my lowest. I want to thank my dad for always having my back and giving me the space to find my way. And I finally I want to thank my partner, Shannon. You make me want to strive to be better.

Appendix

Appendix 1 Media

Table 1. General growth media for *E. coli* and antibiotic stocks used in this project.

General media/stock	Composition	Concentration
LB media autoclaved	Peptone	10 g/l
	Yeast extract	5 g/l
	NaCl	5 g/l
	Demineralised water	Solvent
LB agar autoclaved	Agar	15 g/l
	Peptone	10 g/l
	Yeast extract	5 g/l
	NaCl	5 g/l
	Antibiotic resistance	Variable
	Demineralised water	Solvent
Chloramphenicol stock 1/1000 filter sterilised	Chloramphenicol	34 mg/ml
	Ethanol 100%	Solvent
Streptomycin stock 1/1000 filter sterilised	Streptomycin	50 mg/ml
	MilliQ	Solvent
Kanamycin stock 1/1000 filter sterilised	Kanamycin	50 mg/ml
	MilliQ	Solvent

Table 2. MOPS media 1x recipe

MOPS media	Stocks	Volume (1000 ml)
MOPS media recipe (Neidhardt et al., 1974) Filter sterilised	10X MOPS mixture	100 ml
	0.132 M K_2HPO_4	10 ml
	milliQ H_2O (autoclaved)	880 ml
	7.2 pH (adjusted with NaOH)	~300 µl
	2M $C_6H_{12}O_6$	10 ml

Table 3. 10X MOPS media preparation.

Order	10X MOPS media	Composition	Concentration
1.	Autoclaved, start with 300 ml	Demineralised water	Solvent
2.	Final volume is 1000 ml	MOPS	400 mM
3.	Stored at room temperature	Tricine	40 mM
4.	Add until pH 7.4	KOH	10M
5.	Make fresh	$FeSO_4 \cdot 7H_2O$	10 mM
6.	Mix the following 7 steps in order	NH_4Cl	95 mM
7.		K_2SO_4	2.76 mM
8.		$CaCl_2 \cdot 2H_2O$	5 mM
9.		$MgCl_2$	5.25 mM
10.		NaCl	500 mM
11.	Add 0.2 ml micronutrient stock		
	Micronutrient stock 5000x Filter sterilised Final volume 50 ml	$(NH_4)_6Mo_7O_{24} \cdot 4H_2O$	0.146 mM
		H_3BO_3	20.1 mM
		$CoCl_2$	1.5 mM
		$CuSO_4$	0.48 mM
		$MnCl_2$	4.05 mM
		$ZnSO_4$	0.487 mM
12.	Autoclaved separately	K_2HPO_4 100x	132 mM
13.	Volume finished to 1000 ml and filter sterilize	Demineralised water	Solvent

Table 4. M9 minimal media recipe 1x.

Recipe M9 minimal media	**Composition**	**Amount**
Autoclaved	5X M9 solution mix	200 ml
Filter sterilised	100X trace element mix	10 ml
Autoclaved	1M $MgSO_4$	2 ml
Autoclaved	1M $CaCl_2$	100 ul
Filter sterilised	2M glucose	10 ml
Filter sterilised	0.5 formate	10 ml
Autoclaved	Demiwater H_2O	Fill until 1L

Table 5. M9 minimal media stock preparation.

M9 media stocks (Yishai et al., 2017)	**Composition**	**Concentration**
M9 5X salts Autoclaved	K_2HPO_4	100 mM
	Na_2HPO_4	250 mM
	NaCl	5 mM
	NH_4Cl	100 mM
Mineral mix 100X Filter sterilised	EDTA	13.4 mM
	$FeCl_3 \cdot 6H_2O$	1.3 mM
	$ZnCl_2$	620 µM
	$CuCl_2 \cdot 2H_2O$	760 µM
	$CoCl_2 \cdot 2H_2O$	420 µM
	H_3BO_3	162 µM
	$MnCl_2 \cdot 4H_2O$	8.1 µM
Filter sterilised, carbon source	Glucose	2 M
Filter sterilised, auxotrophy	Formate	0.5 M
Autoclaved	$MgSO_4$	1M
Autoclaved	$CaCl_2$	1M
Autoclaved	Demineralised water	Solvent

Appendix 2 Strains

Table 6. *E. coli* strains used in this project.

Strain name	Description	Original strain	Antibiotic resistance	Genes deleted/mutated	Genes added	Source
K-12 MG1655	Wild type (WT)	W1485	-	*Rph*, *pyrE*, *ilvG*	*Rfb-50* IS5 insertion	(Blattner et al., 1997)
DH5α	Cloning strain	K-12	-	*recA1*, *endA, lacZ*ΔM15		(Glover, 1985)
C1Saux	Formaldehyde dependant growth	MG1655	SmR	*Δ*glyA, *Δ*gcvTHP, *ΔserA, ΔgcvTHP*	*FTL, FolD, GlyA*	(Yishai et al., 2017)
C1Saux-Mdh	C1Saux + pZASSC-rbC-BsMDH	C1Saux	SmR		Mdh (*Bacillus stearothermophilus*)	(Kim et al., 2020)
SM1	Synthetic methylotroph made	BW25113	CmR	*araG, rpoA, xylR, cybB, fhu, ydhB,*	*yggE* to *yghO* 4-fold CNV, *rrsA* to *rrlB* duplicate CNV, *yqiG* to *smf*	(Chen et al., 2020)

	using the RuMP pathway growth			*fdoG, frmA, ugd, smf, gnd, wbbL, stfP, stfE, ΔgapA, gapC, ΔpfkA ΔrpiB, gnd, fdoG, rpoC, proQ, icd, gltA, ptsH, pgi, ptsP, relE, elfG, yhcM*	duplicate CNV, *Medh (Cupriavidus necator)* 2x, *phi (Methylobacillus flagellates)* 2x, *hps (Bacillus methanolicus), hps (Methylomicrobium buryatense), tkt (Methylococcus capsulatus), tal (Klebsiella pneumoniae), gapC (E. coli BL21)*	

Appendix 3 Primers

Table 7. Sequences of primers used in this project.

Primer	Sequence	Target	Size
RV_CmR_tot.F	GGGTCCCCAATAATTACGATTTAAATTGGC	pSEVA331	841
RV_CmR_tot.R	GCAGGGTTATGCAGCGGAAAAG		
RV_pBR322.F	CTTTTCCGCTGCATAACCCTGC	pSEVA291	2419
RV_pBR322.R	ATTTAAATCGTAATTATTGGGGACCCCTGGATTC		
RV-7.F	CGTTTTATTTGATGCCATGCCTCTAGCACGCGTACC	Chap1	1200
RV-7.R	CTAGAGCGGTTCAGTAGAAAAAATACTTGACATATCAC		
RV-8.F	GTATTTTTTCTACTGAACCGCTCTAG	Mdh	1260
RV-8.R	TCAACAGGAGTCCAAGAGTTCGATAGAAACGGCACC		
RV-9.F	CTTGGACTCCTGTTGA	pSEVA391	2680
RV-9.R	GGCATCAAATAAAACG		
RV-22.F	GGTGCCGTTTCTATCGAACTTGGGC	pSEVA391-chap(2-3)	2655
RV-22.R	GATCTATCAACAGGAGTCCAAGTTACATCATGCCG		
RV-23.F	CTTGGACTCCTGTTGATAGATCCAGTAATGACCTCA	pSEVA391-chap1-Mdh	5086
RV-23.R	AGTTCGATAGAAACGGCACCGTGAAC		
RV-24.F	CTTGGACTCCTGTTGATAGATCCAGTAATGACCTC	pSEV2610-sMMO(1-2)	6470
RV-24.R	CGTCGTATGCGTTGCTGTTTACGCTC		
RV-25.F	GGTCATTACTGGATCTATCAACAGGAGTCCAAG	pSEV2610-sMMO(3-4)	2640
RV-25.R	ATGAGCGTAAACAGCAACGCATACGAC		
PS1	AGGGCGGCGGATTTGTCC	AraBAD	Sequencing
PS2	GCGGCAACCGAGCGTTC	MMO C	Sequencing
BG27809	CCAAGTTCAAGGTCGAG	MMO X	Sequencing
BG27810	GCAACTCTCTACTGTT	MMO X	Sequencing

Bibliography

A. J. A. Aarnink, W. J. M. Landman, R. W. Melse, Y. Zhao, J. P. M. Ploegaert, & T. T. T. Huynh. (2011). Scrubber Capabilities to Remove Airborne Microorganisms and Other Aerial Pollutants from the Exhaust Air of Animal Houses. *Transactions of the ASABE*, *54*(5), 1921–1930. https://doi.org/10.13031/2013.39833

Anthony, C. (1982). *The biochemistry of methylotrophs*. https://core.ac.uk/download/pdf/82174801.pdf

Arpaia, S., Nicholas, A., Birch, E., Chesson, A., Du Jardin, P., Gathmann, A., Gropp, J., Herman, L., Hoen-Sorteberg, H.-G., Jones, H., Kiss, J., Kleter, G., Lovik, M., Messéan, A., Naegeli, H., Kaare, M., Nielsen, J., Ovesna, J., Perry, N., … Waigmann, E. (2015). Guidance for renewal applications of genetically modified food and feed authorised under Regulation (EC) No 1829/2003. *EFSA Journal*, *13*(6), 4129. https://doi.org/10.2903/J.EFSA.2015.4129

Baani, M., & Liesack, W. (2008). Two isozymes of particulate methane monooxygenase with different methane oxidation kinetics are found in Methylocystis sp. strain SC2. *Proceedings of the National Academy of Sciences of the United States of America*, *105*(29), 10203–10208. https://doi.org/10.1073/PNAS.0702643105/SUPPL_FILE/ZPQ699084038P.PDF

Bakker, J., Drinkwaard, A., van Doorn, S., Vlugt, S., Poli, D., Marta, P., Pouw, M., Van der vliet, R., Roersma, T., & Lems, S. (2021). *Team:Wageningen UR - 2021.igem.org*. https://2021.igem.org/Team:Wageningen_UR

Bar-Even, A. (2016). Formate Assimilation: The Metabolic Architecture of Natural and Synthetic Pathways. *Biochemistry*, *55*(28), 3851–3863. https://doi.org/10.1021/ACS.BIOCHEM.6B00495/ASSET/IMAGES/MEDIUM/BI-2016-004956_0015.GIF

Bennett, R. K., Dzvova, N., Dillon, M., Jones, S., Hestmark, K., Zhu, B., Helman, N., Greenfield, D., Clarke, E., & Papoutsakis, E. T. (2021). Expression of soluble methane monooxygenase in Escherichia coli enables methane conversion. *BioRxiv*, 2021.08.05.455234. https://doi.org/10.1101/2021.08.05.455234

Bennett, R. K., Gregory, G. J., Gonzalez, J. E., Har, J. R. G., Antoniewicz, M. R., & Papoutsakis, E. T. (2021). Improving the Methanol Tolerance of an Escherichia coli Methylotroph via Adaptive Laboratory Evolution Enhances Synthetic Methanol Utilization. *Frontiers in Microbiology*, *12*. https://doi.org/10.3389/FMICB.2021.638426/FULL

Bennett, R. K., Steinberg, L. M., Chen, W., & Papoutsakis, E. T. (2018). Engineering the bioconversion of methane and methanol to fuels and chemicals in native and synthetic methylotrophs. *Current Opinion in Biotechnology*, *50*, 81–93. https://doi.org/10.1016/J.COPBIO.2017.11.010

Bermejo, L. L., Welker, N. E., & Papoutsakis, E. T. (1998). Expression of Clostridium acetobutylicum ATCC 824 genes in Escherichia coli for acetone production and acetate detoxification. *Applied and Environmental Microbiology*, *64*(3), 1079–1085. https://doi.org/10.1128/AEM.64.3.1079-1085.1998/ASSET/057C95E2-4FA9-4629-8D54-71E42D35DC68/ASSETS/GRAPHIC/AM0381159003.JPEG

Birol, D. F. (2021). *COP26 climate pledges could help limit global warming to 1.8 °C, but implementing them will be the key*. IEA: International Energy Agency.

Blattner, F. R., Plunkett, G., Bloch, C. A., Perna, N. T., Burland, V., Riley, M., Collado-Vides, J., Glasner, J. D., Rode, C. K., Mayhew, G. F., Gregor, J., Davis, N. W., Kirkpatrick, H. A., Goeden, M. A., Rose, D. J., Mau, B., & Shao, Y. (1997). The complete genome sequence of Escherichia coli K-12. *Science (New York, N.Y.)*, *277*(5331), 1453–1462. https://doi.org/10.1126/SCIENCE.277.5331.1453

Burch, D. E., & Williams, D. (1962). Total Absorptance of Carbon Monoxide and Methane in the Infrared. *Applied Optics, Vol. 1, Issue 5, Pp. 587-594*, *1*(5), 587–594. https://doi.org/10.1364/AO.1.000587

Cáceres, M., Dorado, A. D., Gentina, J. C., & Aroca, G. (2017). Oxidation of methane in biotrickling filters inoculated with methanotrophic bacteria. *Environmental Science and Pollution Research International*, *24*(33), 25702–25712. https://doi.org/10.1007/S11356-016-7133-Z

Chen, F. Y. H., Jung, H. W., Tsuei, C. Y., & Liao, J. C. (2020). Converting Escherichia coli to a Synthetic Methylotroph Growing Solely on Methanol. *Cell*, *182*(4), 933--946.e14. https://doi.org/10.1016/j.cell.2020.07.010

Chen, Q., & Ni, J. (2011). Heterotrophic nitrification-aerobic denitrification by novel isolated bacteria. *Journal of Industrial Microbiology & Biotechnology*, *38*(9), 1305–1310. https://doi.org/10.1007/S10295-010-0911-6

Cookney, J., Mcleod, A., Mathioudakis, V., Ncube, P., Soares, A., Jefferson, B., & McAdam, E. J. (2016). Dissolved methane recovery from anaerobic effluents using hollow fibre membrane contactors. *Journal of Membrane Science*, *502*, 141–150. https://doi.org/10.1016/J.MEMSCI.2015.12.037

Cotton, C. A. R., Claassens, N. J., Benito-Vaquerizo, S., & Bar-Even, A. (2020). Renewable methanol and formate as microbial feedstocks. *Current Opinion in Biotechnology*, *62*, 168–180. https://doi.org/10.1016/j.copbio.2019.10.002

de Haas, Y., Veerkamp, R. F., de Jong, G., & Aldridge, M. N. (2021). Selective breeding as a mitigation tool for methane emissions from dairy cattle. *Animal*, *15*, 100294. https://doi.org/10.1016/J.ANIMAL.2021.100294

Dedysh, S. N., & Knief, C. (2018). Diversity and phylogeny of described aerobic methanotrophs. *Methane Biocatalysis: Paving the Way to Sustainability*, 17–42. https://doi.org/10.1007/978-3-319-74866-5_2

Dijkstra, J., Oenema, O., & Bannink, A. (2011). Dietary strategies to reducing N excretion from cattle: implications for methane emissions. *Current Opinion in Environmental Sustainability*, *3*(5), 414–422. https://doi.org/10.1016/J.COSUST.2011.07.008

Drinkwaard, A. (2021). *Team:Wageningen UR/Model/Biofilter - 2021.igem.org*. https://2021.igem.org/Team:Wageningen_UR/Model/Biofilter

Favre, H., & Powell, W. (2013). Front Matter. *Nomenclature of Organic Chemistry*, P001–P004. https://doi.org/10.1039/9781849733069-FP001

Getabalew, M., Alemneh, T., & Akeberegn, D. (2019). *Methane Production in Ruminant Animals: Implication for Their Impact on Climate Change*. https://doi.org/10.32474/CDVS.2019.02.000142

Gibson, B., Wilson, D. J., Feil, E., & Eyre-Walker, A. (2018). The distribution of bacterial doubling times in the wild. *Proceedings of the Royal Society B: Biological Sciences*, *285*(1880). https://doi.org/10.1098/RSPB.2018.0789

Glover, D. M. (1985). *DNA cloning: a practical approach. Volume 1*.

Gregory, G. J., Bennett, R. K., & Papoutsakis, E. T. (2022). Recent advances toward the bioconversion of methane and methanol in synthetic methylotrophs. *Metabolic Engineering*, *71*, 99–116. https://doi.org/10.1016/J.YMBEN.2021.09.005

Grenier, F., Matteau, D., Baby, V., & Rodrigue, S. (2014). Complete Genome Sequence of Escherichia coli BW25113. *Genome Announcements*, *2*(5). https://doi.org/10.1128/GENOMEA.01038-14

Guerrero-Cruz, S., Vaksmaa, A., Horn, M. A., Niemann, H., Pijuan, M., & Ho, A. (2021). Methanotrophs: Discoveries, Environmental Relevance, and a Perspective on Current and Future Applications. *Frontiers in Microbiology*, *12*, 1057. https://doi.org/10.3389/FMICB.2021.678057/XML/NLM

Heux, S., Brautaset, T., Vorholt, J. A., Wendisch, V. F., & Portais, J. C. (2018). Synthetic methylotrophy: Past, present, and future. *Methane Biocatalysis: Paving the Way to Sustainability*, 133–151. https://doi.org/10.1007/978-3-319-74866-5_9/COVER

Hinrichs, K. U., Hayes, J. M., Sylva, S. P., Brewert, P. G., & DeLong, E. F. (1999). Methane-consuming archaebacteria in marine sediments. *Nature*, *398*(6730), 802–805. https://doi.org/10.1038/19751

Howarth, R. W. (2014). A bridge to nowhere: methane emissions and the greenhouse gas footprint of natural gas. *Energy Science & Engineering*, *2*(2), 47–60. https://doi.org/10.1002/ESE3.35

Hungate, R. E. (1967). Hydrogen as an intermediate in the rumen fermentation. *Archiv Für Mikrobiologie 1967 59:1*, *59*(1), 158–164. https://doi.org/10.1007/BF00406327

Idalia, V.-M. N., & Bernardo, F. (2017). *Escherichia coli* as a Model Organism and Its Application in Biotechnology. Escherichia Coli - *Recent Advances on Physiology, Pathogenesis and Biotechnological Applications*. https://doi.org/10.5772/67306

Jakobsen, Ø. M., Benichou, A., Flickinger, M. C., Valla, S., Ellingsen, T. E., & Brautaset, T. (2006). Upregulated transcription of plasmid and chromosomal ribulose monophosphate pathway genes is critical for methanol assimilation rate and methanol tolerance in the methylotrophic bacterium Bacillus methanolicus. *Journal of Bacteriology*, *188*(8), 3063–3072. https://doi.org/10.1128/JB.188.8.3063-3072.2006

JOHNSON, E. D., WOOD, A. S., STONE, J. B., & JR., E. T. M. (2011). SOME EFFECTS OF METHANE INHIBITION IN RUMINANTS (STEERS). *Https://Doi.Org/10.4141/Cjas72-083*, *52*(4), 703–712. https://doi.org/10.4141/CJAS72-083

Johnson, H. D. (1965). Environmental temperature and lactation (with special reference to cattle). *International Journal of Biometeorology*, *9*(2), 103–116. https://doi.org/10.1007/BF02188466/METRICS

Keller, P., Reiter, M. A., Kiefer, P., Gassler, T., Hemmerle, L., Christen, P., Noor, E., & Vorholt, J. A. (2022). Generation of an Escherichia coli strain growing on methanol via the ribulose monophosphate cycle. *Nature Communications 2022 13:1*, *13*(1), 1–13. https://doi.org/10.1038/s41467-022-32744-9

Kim, H. J., Huh, J., Kwon, Y. W., Park, D., Yu, Y., Jang, Y. E., Lee, B. R., Jo, E., Lee, E. J., Heo, Y., Lee, W., & Lee, J. (2019). Biological conversion of methane to methanol through genetic reassembly of native catalytic domains. *Nature Catalysis*, *2*(4), 342–353. https://doi.org/10.1038/s41929-019-0255-1

Kim, J., Kim, D. H. D., & Yoon, S. (2018). Rapid isolation of fast-growing methanotrophs from environmental samples using continuous cultivation with gradually increased dilution rates. *Applied Microbiology and Biotechnology*, *102*(13), 5707–5715. https://doi.org/10.1007/S00253-018-8978-5

Kim, S., Lindner, S. N., Aslan, S., Yishai, O., Wenk, S., Schann, K., & Bar-Even, A. (2020). Growth of E. coli on formate and methanol via the reductive glycine pathway. *Nature Chemical Biology*, *16*(5), 538–545. https://doi.org/10.1038/s41589-020-0473-5

Kim, T. G., Jeong, S. Y., & Cho, K. S. (2014). Functional rigidity of a methane biofilter during the temporal microbial succession. *Applied Microbiology and Biotechnology*, *98*(7), 3275–3286. https://doi.org/10.1007/S00253-013-5371-2/METRICS

Kirschke, S., Bousquet, P., Ciais, P., Saunois, M., Canadell, J. G., Dlugokencky, E. J., Bergamaschi, P., Bergmann, D., Blake, D. R., Bruhwiler, L., Cameron-Smith, P., Castaldi, S., Chevallier, F., Feng, L., Fraser, A., Heimann, M., Hodson, E. L., Houweling, S., Josse, B., … Zeng, G. (2013). Three decades of global methane sources and sinks. *Nature Geoscience*, *6*(10), 813–823. https://doi.org/10.1038/NGEO1955

Krog, A., Heggeset, T. M. B., Müller, J. E. N., Kupper, C. E., Schneider, O., Vorholt, J. A., Ellingsen, T. E., & Brautaset, T. (2013). Methylotrophic Bacillus methanolicus Encodes Two Chromosomal and One Plasmid Born NAD+ Dependent Methanol Dehydrogenase Paralogs with Different Catalytic and Biochemical Properties. *PLOS ONE*, *8*(3), e59188. https://doi.org/10.1371/JOURNAL.PONE.0059188

La, H., Hettiaratchi, J. P. A., Achari, G., & Dunfield, P. F. (2018). Biofiltration of methane. *Bioresource Technology*, *268*, 759–772. https://doi.org/10.1016/J.BIORTECH.2018.07.043

Lai, H. W. H., Benedetti, F. M., Ahn, J. M., Robinson, A. M., Wang, Y., Pinnau, I., Smith, Z. P., & Xia, Y. (2022). Hydrocarbon ladder polymers with ultrahigh permselectivity for membrane gas separations. *Science*, *375*(6587), 1390–1392. https://doi.org/10.1126/SCIENCE.ABL7163/SUPPL_FILE/SCIENCE.ABL7163_MOVIE_S1.ZIP

Li, M. M. J., & Tsang, S. C. E. (2018). Bimetallic catalysts for green methanol production via CO2 and renewable hydrogen: a mini-review and prospects. *Catalysis Science & Technology*, *8*(14), 3450–3464. https://doi.org/10.1039/C8CY00304A

Martínez-García, E., Goñi-Moreno, A., Bartley, B., McLaughlin, J., Sánchez-Sampedro, L., Pascual Del Pozo, H., Prieto Hernández, C., Marletta, A. S., De Lucrezia, D., Sánchez-Fernández, G., Fraile, S., & De Lorenzo, V. (2020). SEVA 3.0: An update of the Standard European Vector Architecture for enabling portability of genetic constructs among diverse bacterial hosts. *Nucleic Acids Research*, *48*(D1), D1164--D1170. https://doi.org/10.1093/nar/gkz1024

Melse, R. W., & Van Der Werf, A. W. (2005). Biofiltration for mitigation of methane emission from animal husbandry. *Environmental Science & Technology*, *39*(14), 5460–5468. https://doi.org/10.1021/ES048048Q

Morgavi, D. P., Forano, E., Martin, C., & Newbold, C. J. (2010). Microbial ecosystem and methanogenesis in ruminants. *Animal*, *4*(7), 1024–1036. https://doi.org/10.1017/S1751731110000546

Moser, J. W., Prielhofer, R., Gerner, S. M., Graf, A. B., Wilson, I. B. H., Mattanovich, D., & Dragosits, M. (2017). Implications of evolutionary engineering for growth and recombinant protein production in methanol-based growth media in the yeast Pichia pastoris. *Microbial Cell Factories*, *16*(1), 1–16. https://doi.org/10.1186/S12934-017-0661-5/FIGURES/3

Myrhe, G., & Shindell, D. (2013). Anthropogenic and Natural Radiative Forcing BT - Climate Change 2013: The Physical Science Basis. *Climate Change 2013: The Physical Science Basis*, *8*, 1–141. papers3://publication/uuid/3FE291E6-1236-4CF0-9EC2-83D39F6664FF

Nakamura, J., & Nakamura, M. (2020). DNA-protein crosslink formation by endogenous aldehydes and AP sites. *DNA Repair*, *88*, 102806. https://doi.org/10.1016/J.DNAREP.2020.102806

Neidhardt, F. C., Bloch, P. L., & Smith, D. F. (1974). Culture medium for enterobacteria. *Journal of Bacteriology*, *119*(3), 736–747. https://doi.org/10.1128/JB.119.3.736-747.1974

Neidhardt, F. C., Ingraham, J. L., & Schaechter, M. (1990). Physiology of the bacterial cell. A molecular approach. By F C Neidhardt, J L Ingraham and M Schaechter. pp 507. Sinauer associates, Sunderland, MA. 1990. $43.95 ISBN 0–87893–608–4. *Biochemical Education*, *20*(2), 124–125. https://doi.org/10.1016/0307-4412(92)90139-D

Nguyen, A. D., Hwang, I. Y., Chan, J. Y., & Lee, E. Y. (2016). Reconstruction of methanol and formate metabolic pathway in non-native host for biosynthesis of chemicals and biofuels. *Biotechnology and Bioprocess Engineering 2016 21:4*, *21*(4), 477–482. https://doi.org/10.1007/S12257-016-0301-7

Norris, F., Norris, P., Gundry, T., & Jones, C. (2023). *US Patent Application for METHANE OXIDATION DEVICE Patent Application (Application #20230390698 issued December 7, 2023) - Justia Patents Search*. https://patents.justia.com/patent/20230390698

Novikov, V. V., & Stepanov, A. L. (2002). Coupling of Microbial Processes of Methane and Ammonium Oxidation in Soils. *Microbiology 2002 71:2*, *71*(2), 234–237. https://doi.org/10.1023/A:1015166708940

Nowakowicz-Debek, B., Wlazło, Ł., Szymula, A., Ossowski, M., Kasela, M., Chmielowiec-Korzeniowska, A., & Bis-Wencel, H. (2020). Estimating Methane Emissions from a Dairy Farm Using a Computer Program. *Atmosphere 2020, Vol. 11, Page 803*, *11*(8), 803. https://doi.org/10.3390/ATMOS11080803

Olivier, J. G. J., & Peters, J. A. H. W. (2020). *TRENDS IN GLOBAL CO 2 AND TOTAL GREENHOUSE GAS EMISSIONS 2019 Report*. https://www.pbl.nl/sites/default/files/downloads/pbl-2020-trends-in-global-

Pereira, A. M., De Lurdes Nunes, M., Dapkevicius, E., & Borba, A. E. S. (2022). Alternative pathways for hydrogen sink originated from the ruminal fermentation of carbohydrates: Which microorganisms are involved in lowering methane emission? *Animal Microbiome 2022 4:1*, *4*(1), 1–12. https://doi.org/10.1186/S42523-021-00153-W

Ranganathan, J., Waite, R., Searchinger, T., & Hanson, C. (2018). *How to Sustainably Feed 10 Billion People by 2050, in 21 Charts*. https://www.wri.org/insights/how-sustainably-feed-10-billion-people-2050-21-charts

Reeburgh, W. S. (2007). Oceanic methane biogeochemistry. *Chemical Reviews*, *107*(2), 486–513. https://doi.org/10.1021/CR050362V/ASSET/CR050362V.FP.PNG_V03

Ross, M. O., & Rosenzweig, A. C. (2017). A tale of two methane monooxygenases. *Journal of Biological Inorganic Chemistry : JBIC : A Publication of the Society of Biological Inorganic Chemistry*, *22*(2–3), 307–319. https://doi.org/10.1007/S00775-016-1419-Y

Sanford, P. A., & Woolston, B. M. (2022). Synthetic or natural? Metabolic engineering for assimilation and valorization of methanol. *Current Opinion in Biotechnology*, *74*, 171–179. https://doi.org/10.1016/J.COPBIO.2021.12.001

Singh, H. B., Kang, M. K., Kwon, M., & Kim, S. W. (2022). Developing methylotrophic microbial platforms for a methanol-based bioindustry. *Frontiers in Bioengineering and Biotechnology*, *10*, 1050740. https://doi.org/10.3389/FBIOE.2022.1050740/BIBTEX

Sirajuddin, S., & Rosenzweig, A. C. (2015). Enzymatic oxidation of methane. *Biochemistry*, *54*(14), 2283–2294. https://doi.org/10.1021/acs.biochem.5b00198

Spranger, T. M. (2015). *Legal Analysis of the applicability of Directive 2001/18/EC on genome editing technologies*.

Stolyar, S., Costello, A. M., Peeples, T. L., & Lidstrom, M. E. (1999). Role of multiple gene copies in particulate methane monooxygenase activity in the methane-oxidizing bacterium Methylococcus capsulatus Bath. *Microbiology (Reading, England)*, *145 (Pt 5)*(5), 1235–1244. https://doi.org/10.1099/13500872-145-5-1235

Sun, M. T., Zhao, Y. Z., Yang, Z. M., Shi, X. S., Wang, L., Dai, M., Wang, F., & Guo, R. B. (2020). Methane Elimination Using Biofiltration Packed With Fly Ash Ceramsite as Support Material. *Frontiers in Bioengineering and Biotechnology*, *8*, 351. https://doi.org/10.3389/FBIOE.2020.00351/BIBTEX

Thakur, C. S., Brown, M. E., Sama, J. N., Jackson, M. E., & Dayie, T. K. (2010). Growth of wildtype and mutant E. coli strains in minimal media for optimal production of nucleic acids for preparing labeled nucleotides. *Applied Microbiology and Biotechnology*, *88*(3), 771. https://doi.org/10.1007/S00253-010-2813-Y

Ungerfeld, E. M. (2020). Metabolic Hydrogen Flows in Rumen Fermentation: Principles and Possibilities of Interventions. *Frontiers in Microbiology*, *11*, 589. https://doi.org/10.3389/FMICB.2020.00589/BIBTEX

Val-Laillet, D., Guesdon, V., von Keyserlingk, M. A. G., de Passillé, A. M., & Rushen, J. (2009). Allogrooming in cattle: Relationships between social preferences, feeding displacements and social dominance. *Applied Animal Behaviour Science*, *116*(2–4), 141–149. https://doi.org/10.1016/J.APPLANIM.2008.08.005

Valle, A., & Bolívar, J. (2021). Escherichia coli, the workhorse cell factory for the production of chemicals. *Microbial Cell Factories Engineering for Production of Biomolecules*, 115–137. https://doi.org/10.1016/B978-0-12-821477-0.00012-X

Vallero, D. A. (2019). Air pollution biogeochemistry. *Air Pollution Calculations*, 175–206. https://doi.org/10.1016/B978-0-12-814934-8.00008-9

van Amstel, A. (2012). Methane. A review. In *Journal of Integrative Environmental Sciences*. https://doi.org/10.1080/1943815X.2012.694892

van Breukelen, A. E., Aldridge, M. A., Veerkamp, R. F., & de Haas, Y. (2022). Genetic parameters for repeatedly recorded enteric methane concentrations of dairy cows. *Journal of Dairy Science*, *105*(5). https://doi.org/10.3168/JDS.2021-21420

van der Zaag, A. C., Flesch, T. K., Desjardins, R. L., Baldé, H., & Wright, T. (2014). Measuring methane emissions from two dairy farms: Seasonal and manure-management effects. *Agricultural and Forest Meteorology*, *194*, 259–267. https://doi.org/10.1016/J.AGRFORMET.2014.02.003

van Lingen, H. J., Fadel, J. G., Yáñez-Ruiz, D. R., Kindermann, M., & Kebreab, E. (2021). Inhibited Methanogenesis in the Rumen of Cattle: Microbial Metabolism in Response to Supplemental 3-Nitrooxypropanol and Nitrate. *Frontiers in Microbiology*, *12*. https://doi.org/10.3389/FMICB.2021.705613

Wang, W., Iacob, R. E., Luoh, R. P., Engen, J. R., & Lippard, S. J. (2014). Electron transfer control in soluble methane monooxygenase. *Journal of the American Chemical Society*, *136*(27), 9754–9762. https://doi.org/10.1021/JA504688Z/SUPPL_FILE/JA504688Z_SI_001.PDF

Wenk, S., Schann, K., He, H., Rainaldi, V., Kim, S., Lindner, S. N., & Bar-Even, A. (2020). An “energy-auxotroph” Escherichia coli provides an in vivo platform for assessing NADH regeneration systems. *Biotechnology and Bioengineering*, *117*(11), 3422–3434. https://doi.org/10.1002/BIT.27490

Wilkinson, J. M. (2012). Methane production by ruminants. *Livestock*, *17*(4), 33–35. https://doi.org/10.1111/J.2044-3870.2012.00125.X

Woo, J. E., Seong, H. J., Lee, S. Y., & Jang, Y. S. (2019). Metabolic Engineering of Escherichia coli for the Production of Hyaluronic Acid From Glucose and Galactose. *Frontiers in Bioengineering and Biotechnology*, *7*. https://doi.org/10.3389/FBIOE.2019.00351

Wu, L. (2016). *Measurement Methods to Assess Methane Production of Individual Dairy Cows in a Barn*.

Yishai, O., Goldbach, L., Tenenboim, H., Lindner, S. N., & Bar-Even, A. (2017). Engineered Assimilation of Exogenous and Endogenous Formate in Escherichia coli. *ACS Synthetic Biology*, *6*(9), 1722–1731. https://doi.org/10.1021/acssynbio.7b00086

Yurimoto, H., Oku, M., & Sakai, Y. (2011). Yeast methylotrophy: Metabolism, gene regulation and peroxisome homeostasis. *International Journal of Microbiology*. https://doi.org/10.1155/2011/101298